

# Contribution of Theoretical Chemistry to the Study of Ion Transport through Membranes

A. PULLMAN

*Institut de Biologie Physico-Chimique, (Fondation Edmond de Rothschild) 13, rue Pierre et Marie Curie, 75005 Paris, France**Received November 21, 1990 (Revised Manuscript Received May 3, 1991)*

## Contents

I. Introduction	793
II. Ionophores	795
III. Channel-Making Antibiotics	798
A. Gramicidin A	798
1. Energy Profiles	799
2. Water Structure	801
3. Water and Ions	801
4. Flexibility and Librations	802
5. Helix Handedness	802
6. Other Structures	802
B. Alamethicin and Macrolide Channels	803
IV. Ion Channels in Membrane Proteins	803
A. Bundles of Hydrophobic $\alpha$ -Helices	803
1. Pairing Properties of Hydrophobic Helices of Increasing Length	804
2. Bundles of <i>N</i> Hydrophobic $\alpha$ -Helices	805
3. The Capacity of a Purely Hydrophobic Bundle To Act as Ion Channel. Role of Polar Residues	806
B. Building of a Model of a Physiological Channel: The Nicotinic Acetylcholine Receptor Channel	806
1. Shape and Dimensions of the Model	807
2. The Limits of the Helices and the Role of the Charged Residues	808
3. The Role of the Other Helices	808
4. Energy Profiles in Mutants as Confirmation of the Overall Model	809
V. Concluding Remarks	809
VI. References	809

## I. Introduction

Biological membranes surround the cells and their various compartments. They maintain the different domains within limits but also allow proper communication between them when needed, insuring the appropriate in-and-out flux of molecules and ions necessary for the functioning of the cell machinery.<sup>1</sup> The basic structure of these membranes<sup>2,3</sup> consists of a layer of hydrocarbon chains topped with "polar heads". The chains pack side by side along their long axis so as to form a layer with all the polar heads adjacent to each other, and two such layers form a tail-to-tail bilayer (Figure 1). Although the length and precise chemical composition of the hydrocarbon chains varies in different membranes as do also polar heads (cf. Figure 2), the general characteristics described above are conserved throughout the membrane world. It is clear that, due to their lipidic constitution, membranes cannot be easily crossed without assistance by the largely polar or ionic species which constitute the main part of the



Alberte Pullman was born in Nantes, France and grew up in Paris. She studied at the Sorbonne and became Licenciée es Sciences Physiques in 1943. A student of Louis de Broglie, she started research at the Institut du Radium and became Docteur es Sciences in 1946 with a thesis on the correlation between the electronic structure and the carcinogenic activity of aromatic compounds. She performed her whole career at the CNRS (the National Research Council of France) where she has held the position of Research Director since 1963. She is a member since 1968, past Vice-President (1979-85), and presently President of the International Academy of Quantum Molecular Science, Doctor Honoris causa of the Universities of Liège (Belgium), Uppsala (Sweden), and Torino (Italy), Vice-President and then President of the International Society of Quantum Biology, recipient of the Essec Prize of the French Ligue against Cancer, of the Louis Bonneau, of the Charles Louis de Saules de Freycinet, and of the Atomic Energy Commission Prizes of the French Academy of Sciences, and of the Cori Award of the Roswell Park Memorial Institute. She is a Knight of the Legion of Honor and officier of the French National Order of Merit. Her research interests have covered practically all aspects of theoretical chemistry as applied to the understanding of molecular properties, with an ever-increasing accent on biochemical compounds. Coauthor of three books with Bernard Pullman, and author of over 300 publications, she has devoted her interest in the recent years to the problem of ion transport in biological membranes.

cellular traffic. Thus, in order to insure that the appropriate transport takes place through the various membranes at the time when it is needed, nature uses specialized molecules, the membrane proteins, which are "integrated", totally or partially, in the membranes<sup>4</sup> (Figure 3) and which provide, within their macromolecular structure, a device—channel, carrier, or pump—allowing the polar or ionic species to transit, sheltered from the lipid phase by the surrounding protein.

Channels are essentially tunnels or pores, permanent or transient, with an inner wall sufficiently hydrophilic to allow diffusion of the polar entity according to its concentration gradient. Pumps and carriers bind the ligand on one side and deliver it on the other. Beyond this phenomenological description, the detailed mechanisms involved in each case are still very poorly understood at the molecular level, because of lack of structural information: it was only in the 1970's that

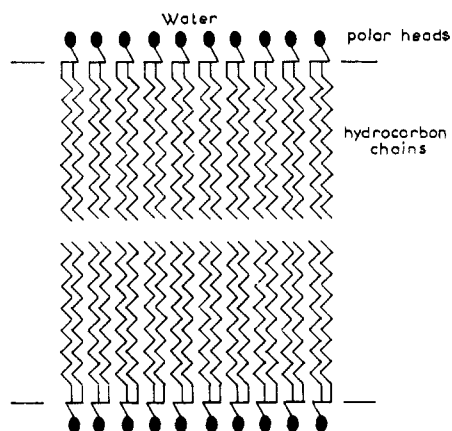


Figure 1. A schematic view of the tail-to-tail arrangement of lipids in membranes.

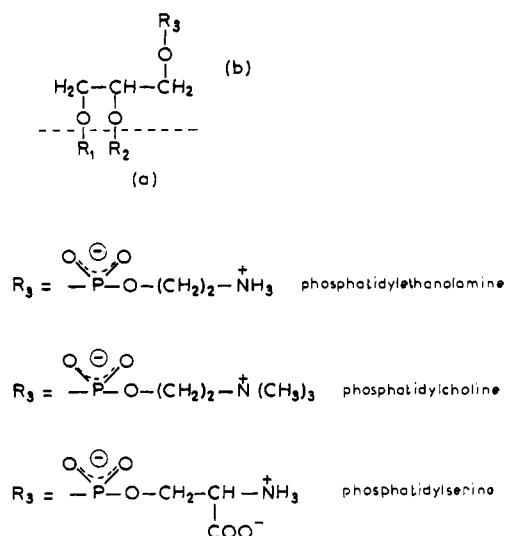


Figure 2. The structure of typical glycerophospholipids: (a) hydrocarbon chains and (b) polar heads. R1, R2 = saturated fatty acid chains  $\text{CH}_3(\text{CH}_2)_n\text{CO}$ ,  $n = 8-22$ ; also mono-, di-, tri-, and tetraunsaturated chains with 16-22 carbon atoms.

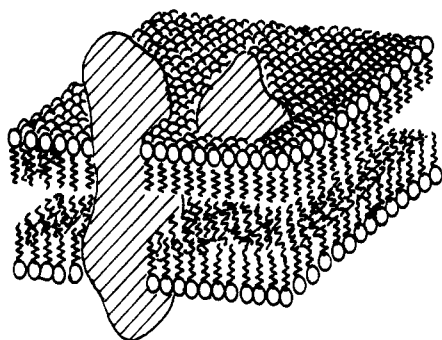


Figure 3. Membrane proteins inserted in the bilayer.

adequate methods of isolation and purification applicable to membrane proteins were developed, allowing the beginning of the identification of their subunit composition and gross architecture. As concerns the ion-transport proteins (to which we shall limit our consideration), the deciphering of their amino acid content began in 1979 with the determination of the entire sequence of bacteriorhodopsin<sup>5,6</sup> and of the amino terminal part of the nicotinic acetylcholine receptor,<sup>7,8</sup> followed soon after by the complete sequencing of receptors from different organisms<sup>9</sup> and more recently by

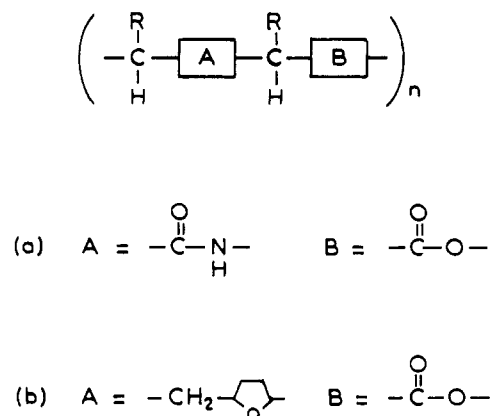


Figure 4. Structural constituents of typical ionophores: (a) depsipeptides, R = lipophilic group; and (b) macroretrolides, R = H (compare to standard polypeptides: A = B = CONH, R = polar or apolar side chains).

that of other ligand-gated receptors.<sup>10-12</sup> To this must be added the sequencing of the voltage-gated sodium,<sup>13</sup> calcium, and potassium<sup>14</sup> channels, of visual rhodopsins,<sup>15,16</sup> of halorhodopsin,<sup>17a</sup> of the anion-specific band-3 protein,<sup>17b</sup> of the major ATP-linked ion pumps,<sup>18,19</sup> etc. (e.g. ref 20). Unfortunately, the structural information necessary to complete the molecular picture of these membrane proteins, namely X-ray diffraction data, have been, until very recently, cruelly lacking, essentially owing to the difficulty encountered for obtaining three-dimensional crystals with appropriate diffracting properties.<sup>21</sup> A recent notable exception is the obtention of high-resolution data on the photosynthetic reaction center of *Rhodospseudomonas viridis*<sup>22</sup> followed by that of *Rhodobacter sphaeroides* (cf. ref 23) (both membrane protein complexes, albeit not ion-transport proteins). Another promising technique in this field appears to be the analysis of electron-scattering density maps obtained from two-dimensional crystals. The refinement of this technique, pioneered in 1975 on the proton pump bacteriorhodopsin,<sup>24</sup> has recently culminated in the production of a structural model at 3.5-Å resolution.<sup>25</sup>

The uncertainties encountered in the structural investigation of ion-transport proteins have delayed considerably the determination of structure-function relationships which could lead to a clear-cut understanding of their mechanism(s) of functioning.

On the other hand, the discovery<sup>26-29</sup> that relatively simple antibiotics induced selective ion conductance in biological and model membranes raised the hope that the study of the behavior of these simple molecules could provide a clue at least to part of the factors involved in ion transfer. These antibiotics are of two kinds: the simplest ones, the "ionophores", or ion carriers, which are low molecular weight substances often, but not necessarily, cyclic, the structure of which is made of a succession of polar groups ( $n = 6-12$ ) separated by at least one saturated carbon atom carrying a lipophilic (generally hydrocarbon) residue (Figure 4). It was early recognized (for instance, ref 30) that this peculiar structure conferred on ionophore antibiotics the ability to form lipid-soluble ionic complexes in which the polar groups are used to capture and engage the ion, taking advantage of the conformational lability due to their single bonds, so as to ensure the formation of the most favorable cavity for a given ion,

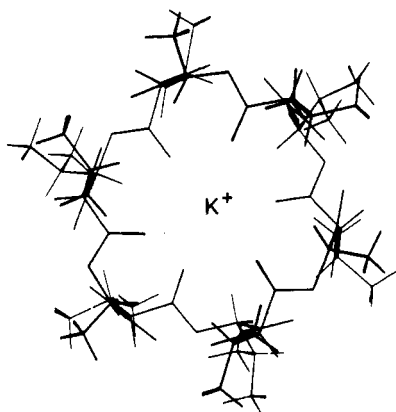
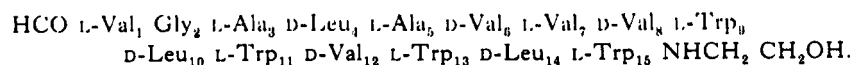


Figure 5. A schematic view of the crystal structure of the potassium complex of valinomycin.

while turning at the same time the lipophilic residues toward the exterior of the complex, thereby allowing a favorable interaction with the lipids. An example of such a complex is given in Figure 5.

This phenomenological description, although containing the fundamental elements governing the action of ionophores, does not describe the detailed mechanisms involved, in particular the capture of the ion, the mode of transport proper (by shuttling or passing over), the ion release, the specificity for a given species, etc. Thus, in the hope of solving these problems, a considerable amount of experimental research developed on the ionophore antibiotics themselves and their analogues,<sup>30-35</sup> to which was soon added the study of their close cousins the crown ethers<sup>36</sup> and the cryptands.<sup>37,38</sup> The excitement produced by the booming experimental developments of the early 1970's inspired at that time the undertaking of theoretical computations which helped both the elaboration of appropriate methodologies and the understanding of the respective roles of the various structural elements in the properties of these compounds and of their complex interplay (cf. section II).

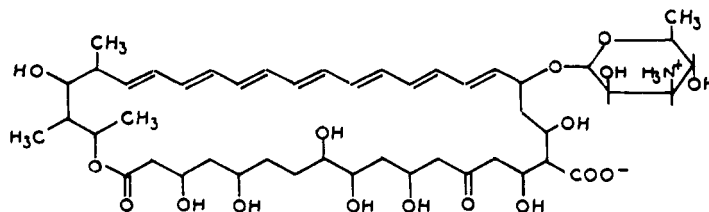
The second kind of antibiotics which induce ion transport through membranes is believed to do so by



(a)



(b)



(c)

Figure 6. The chemical constitution of (a) gramicidin A, (b) alamethicin, and (c) amphotericin B.

forming channels. To this category belongs gramicidin A, a polypeptide made of 15 alternating L and D hydrophobic amino acids<sup>39a</sup> (Figure 6a), alamethicin (Figure 6b) and its analogues,<sup>39b-e</sup> also essentially polypeptidic, with a high content of aminoisobutyric acid, and a group of polyene macrolides typified by amphotericin B (Figure 6c). Gramicidin A utilizes two molecules<sup>40</sup> to form a channel spanning the membrane, most likely by head-to-head association into a continuous  $\beta$ -helix.<sup>41,42</sup> Alamethicin<sup>43-45</sup> and also amphotericin B<sup>46-47</sup> form more complex aggregates of a larger number of units which reorganize into a channel under various conditions. The polypeptidic nature of gramicidin A and alamethicin makes them interesting models for the investigation of the role of the different structural elements involved in the formation and functioning of protein channels in membranes, particularly insofar as these are also polypeptidic. Owing to its relative simplicity and the abundant experimental data, gramicidin A has been an object of choice for theoretical investigations, the outcome of which is summarized in section III.A. Alamethicin and its analogues, abundantly studied by a variety of experimental techniques, have been, altogether, less attractive to theorists until now (cf. section III.B). The relatively scarce theoretical data concerning the polyene macrolides are briefly summarized also in section III.B.

Section IV deals with theoretical studies directly concerned with membrane proteins themselves.

## II. Ionophores

Early calculations on ionophores, devoted to the depsipeptides valinomycin and enniatin B, served to establish the fundamental characteristic properties of two most conspicuous elements of their structure, the degree of rotational flexibility of their single bonds and the cation binding properties of their amide and ester groups. Conformational analysis (empirical<sup>48-51</sup> as well as ab initio<sup>51-52</sup>) showed that the single carbon-heteroatom bond of the ester group has less conformational flexibility than the corresponding bond of amides, a

probably far-reaching indication that the presence of the ester group can impose conformational constraints on the overall structure which may be adopted by the macrocycles. On the other hand, *ab initio* SCF calculations<sup>53a</sup> showed that the intrinsic affinity of the amide carbonyl oxygen for alkali ions was larger than that of an ester carbonyl, itself close to that of the oxygen of water; this result (confirmed appreciably later by measurements of gas-phase enthalpies of binding)<sup>64</sup> suggested<sup>53a</sup> that the lower affinity of an ester carbonyl with respect to that of an amide one was probably one of the factors explaining the intriguing decrease in complex stability observed upon replacement of the *N*-methyl peptide group by an ester group in enniatin B and, conversely, for the increase in complex stability observed upon replacement, in valinomycin, of the L-lactic and D-hydroxyvaleric acid residues by L- and D-prolines, respectively.

Such *ab initio* model studies, carried out for various ligands, were instrumental in determining not only their relative intrinsic affinities, but also the corresponding ion–ligand equilibrium distances, the nature of the binding, the lability with respect to equilibrium, etc., all information which at that time was inaccessible, but indispensable for the determination, on a firm basis<sup>55a</sup> (see also ref 55b), of the parameters of empirical potential functions which were necessary to perform reasonably accurate, feasible computations on the ionophores themselves, the size of which precluded, except for very crude modeling, the utilization of reliable *ab initio* procedures (most all-valence electrons methods are notable<sup>53a,b</sup> for yielding artifacts in the domain of ion–ligand binding). The SIBFA method, including all the components of the theory of intermolecular forces, was developed on this basis.<sup>56</sup> Its utilization in the study of the interaction of alkali cations with valinomycin,<sup>57</sup> of Na<sup>+</sup>, K<sup>+</sup>, and NH<sub>4</sub><sup>+</sup> with nonactin,<sup>58a</sup> and of Mg<sup>2+</sup> and Ca<sup>2+</sup> with the ionophore A23187<sup>59</sup> was the first successful attempt at a delineation of the respective roles of the different components of the complexation energy in the determination of the ionophore's specificity.<sup>60</sup> Even though the qualitative analysis at the phenomenological level had led to enumerate early<sup>30,61a,b</sup> the main factors involved (ion–ionophore interaction energy, desolvation energies, internal energy variation upon complexation), the evaluation of their relative weights in the energy balance remained uncertain,<sup>62,63</sup> essentially for lack of appropriate methodologies. The methodological advances quoted above allowed to go one step further.

In the case of valinomycin (Figure 7a), advantage could be taken of the availability of the crystal structure of its K<sup>+</sup> complex<sup>64</sup> which displays a very characteristic "bracelet-like" conformation where all the amide NH and CO groups form a tight array of hydrogen bonds (Figure 7b), leaving the six ester carbonyls free to "encage" the ion, three above and three below (cf. Figure 5). Assuming tentatively that the overall structure of the cage remained essentially the same in the complexes of the other alkali ions (an assumption justified at the time by the obvious rigidity of the "bracelet" of hydrogen bonds and confirmed recently by molecular mechanics computations, including labilization of the cage<sup>65</sup>), the ion–ionophore interactions calculated for Na<sup>+</sup>, K<sup>+</sup>, Rb<sup>+</sup>, and Cs<sup>+</sup> by energy mini-

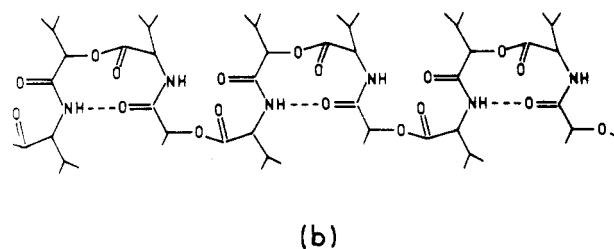
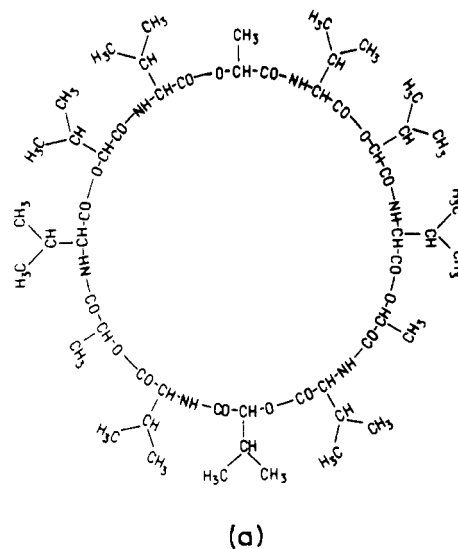


Figure 7. Structural properties of valinomycin: (a) sequence, and (b) the array of NH...OC hydrogen bonds in the "bracelet-like" structure.

mization, allowing the ion to reach its optimal position, indicated that (i) the optimal values of the energies of interactions are in the order Na<sup>+</sup> > K<sup>+</sup> > Rb<sup>+</sup> > Cs<sup>+</sup>, (ii) K<sup>+</sup>, Rb<sup>+</sup>, and Cs<sup>+</sup> prefer an essentially central position in the cavity while Na<sup>+</sup> is shifted from the center to the vicinity of two of the carbonyl oxygens, a result in agreement with those of infrared measurements of the carbonyl frequencies of the Na<sup>+</sup> complex.<sup>66–68</sup> Recently more accurate molecular mechanics computations of the Na<sup>+</sup> complex, including optimization of the cavity,<sup>65</sup> confirmed the theoretical result.

The order found for the ion–ionophore interaction energies is the inverse of the order resulting from the measurements of the binding constants of the complexes in alcoholic solvents, namely:<sup>69,70a</sup> Rb<sup>+</sup> > K<sup>+</sup> > Cs<sup>+</sup> >> Na<sup>+</sup> (Eisenman's selectivity sequence III<sup>70b,c</sup>). Within the hypothesis of a rigid cage, the second most important component of the complexation energy to consider is the desolvation energy of the cation. The values (tentatively taken as the inverse of the available enthalpies of solvation in water<sup>71–73</sup> or in methanol<sup>74</sup>) being in the same order as the ion–ionophore binding energies do not, by themselves, account for the order of the observed complexing abilities. But when the two components are taken into account simultaneously, the order of the energy balance becomes identical with the selectivity order, with K<sup>+</sup> very close to Rb<sup>+</sup>, Cs<sup>+</sup> somewhat behind, and Na<sup>+</sup> much behind as exemplified in Table I. This is true whatever the values adopted for the desolvation enthalpies, even though the nu-

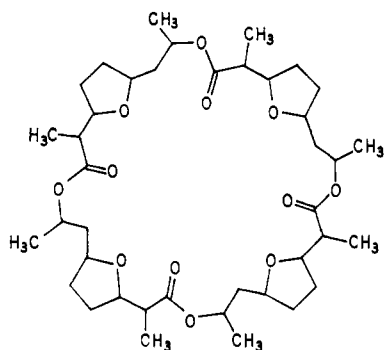
**TABLE I. Energy Balance in the Valinomycin-Cation Complexes (Energies in kcal/mol)**

ion	Na <sup>+</sup>	K <sup>+</sup>	Rb <sup>+</sup>	Cs <sup>+</sup>
$E_i^a$	-108.5	-106.4	-102.7	-88.8
$E_h^b$	106.0	85.8	79.8	72.0
$DE^c$	-2.5	-20.6	-22.9	-16.8
$d^d$	20.4	2.3	0.0	6.1

<sup>a</sup> Interaction energy of the ion with the K<sup>+</sup> cavity.

<sup>b</sup> Experimental desolvation enthalpy (from ref 74). <sup>c</sup>  $E_i + E_h$ .

<sup>d</sup> Difference with respect to the best balance.

**Figure 8.** The nonactin molecule.

merical values of the balance, of course, differ (see Table III in the original paper<sup>57</sup> and the discussion). Thus, in valinomycin it is possible to account for the specificity of the association by taking into consideration solely the complexation and the desolvation energies, the two terms operating in opposite directions but with different differential effects. The fact that the decisive factor in determining the selectivity for K<sup>+</sup> over Na<sup>+</sup> in valinomycin resides in the difference in the desolvation energies of the ions was confirmed by calculations taking into account the deformation of the cage upon complexation<sup>65</sup> (see also similar conclusions obtained with a different force field<sup>75</sup>).

That the relatively simple interplay of the components of the energy balance upon complexation is not necessarily the same for other ionophores was shown by calculations<sup>58a</sup> on nonactin (Figure 8). Like valinomycin this ionophore prefers K<sup>+</sup> to Na<sup>+</sup>. In this case, the crystal structures of both the Na<sup>+</sup> complex<sup>76</sup> and the K<sup>+</sup> complex<sup>77-78</sup> were available, both showing the ion linked to the four carbonyls and the four tetrahydrofuran oxygens in a cavity more contracted in the Na<sup>+</sup> complex than in the K<sup>+</sup> one. The ion-ionophore interaction energy, calculated for each ion in its own cavity, indicates that Na<sup>+</sup> binds much more strongly than K<sup>+</sup>, with a difference in energy appreciably larger than the differences between the corresponding desolvation energies, so that, even though the desolvation energies operate in the right direction for reducing the gap between the two ions, the energy balance remains in the wrong order, favoring Na<sup>+</sup>. But, owing to the more contracted size of the Na<sup>+</sup> cavity with respect to the K<sup>+</sup> one, the ligand-ligand repulsions are appreciably stronger in the Na<sup>+</sup> complex. A tentative approximate evaluation of these terms led to the conclusion that the decisive effect in the K<sup>+</sup>/Na<sup>+</sup> selectivity of nonactin resides in the change of conformation between the two complexes (cf. ref 58 for details). (A similar decisive effect of the conformational energy variation of the ionophore upon complex formation was found to operate in the marked selectivity for Ca<sup>2+</sup> over Mg<sup>2+</sup> of

the ionophore 3,6-dioxaoctanediamide.<sup>79</sup>) The intriguing preference of nonactin for NH<sub>4</sub><sup>+</sup> over K<sup>+</sup><sup>80</sup> was attributed<sup>58a</sup> to the ion-ionophore interaction energies themselves, largely in favor of the ammonium ion, so much that the resulting order is not modified by the introduction of the desolvation energies in the balance. The "cage" deformations are apparently negligible although the two ions bind differently to the different oxygen atoms (see ref 58a-c).

These simple examples illustrate the complexity of the interplay of the different energy components in the complexation selectivity of the ionophores: while the order of the ion-ionophore interaction energies can be decisive, as in the NH<sub>4</sub><sup>+</sup>/K<sup>+</sup> nonactin preference, the reversal of this order can occur either by the sole effect of the desolvation energies, as in valinomycin, or necessitate the conjunction of this effect with that of the conformational energy variations as seen in the K<sup>+</sup>/Na<sup>+</sup> selectivity of nonactin or the calcium/magnesium selectivity of dioxethane dioxamide. Another complex interplay of the binding and conformational energies was also brought into evidence by more recent molecular mechanics calculations including conformational energy optimizations,<sup>81,75</sup> considering the preference of enniatin B for internal or external complexes with alkali ions: the low resulting specificity for external binding as opposed to the more "strained" internal binding was suggested to be in correlation with the relatively low specificity of this depsipeptide compared to that of valinomycin (cf. also ref 65). Another factor in some specificities may be the inclusion of individual water molecules in a complex, as suggested to be the case for the carboxylic ionophore A23187, where water molecules remaining bound to the Ca<sup>2+</sup> complex may tip the energy balance in favor of this ion as compared to the situation in the Mg<sup>2+</sup> complex.<sup>59</sup> The presence of such an internal water molecule inside a bracelet-like cavity has been found<sup>82</sup> in a valinomycin-Na<sup>+</sup>-picrate crystal with Na<sup>+</sup> and picrate outside the cavity (compared to the corresponding K<sup>+</sup>-picrate<sup>83</sup> without water). More complex theoretical decompositions of the components of the energy balance have been made in some cases.<sup>84</sup>

The problem of the specificity for complexation, in relation to the specificity for ion transport, is only one of the numerous problems mentioned in the Introduction concerning the action of the ion carriers. It appears also the one for which theory has been the most active. Neither the difficult problem of the mechanisms intervening in the ion capture and release at the interface, nor that of the transport proper through the lipid phase, have been considered extensively. Worth mentioning are early attempts<sup>85</sup> to utilize molecular electrostatic potentials and atomic accessibilities of an asymmetric, uncomplexed form of valinomycin, detected in a crystal structure<sup>86</sup> to characterize which of the free carbonyl oxygens of the structure are the more apt to initiate the capture of the cation. Apart from this kind of consideration, the more "classical", although still indirect, way of dealing with the mechanism of ion capture or release has been limited to the consideration of the numerous conformational forms, found by molecular mechanics calculations in the complexed and uncomplexed state of a given ionophore, and to the utilization<sup>85,75,81,87,88</sup> of the energetic and structural results in conjunction for deducing an "educated guess" on the possible mecha-

nism(s) of complexation. Still sorely lacking is the explicit inclusion of water in the calculations other than by the tentative introduction of a dielectric constant (cf. ref 65), a notable exception being a Monte Carlo calculation of the hydration of two uncomplexed forms of valinomycin and of its  $K^+$  complex.<sup>89</sup> The results, indicating a much stronger hydration of the open form than of the closed form considered, were used to imagine a model of the succession of events upon complexation and transfer. (See also a brief report of a partial modelization of the ionophore X537A.<sup>90a</sup>)

Molecular dynamics calculations including water at the interface and lipids in the membrane are surprisingly still absent in the field of the ionophore antibiotics, although the problems raised by their functioning, particularly in the transport itself, would seem to be excellent topics for such techniques. Although the studies of crown ethers, cryptands, and model peptides are outside the scope of this review insofar as they do not function in membrane transport, mention must be made of theoretical calculations on these compounds touching problems closely connected with those encountered in the field of ion carriers, most particularly those related to the specificity of complexation. Notable among them are molecular mechanics, Monte Carlo, and dynamics studies of 18-crown-6<sup>90b-d</sup> of typical bicyclic and tricyclic cryptands,<sup>90e-g</sup> and of spherands.<sup>90h</sup> An extension of such computations to the realistic study of the ion carriers at the water-lipid interface and of the dynamics of their interactions within the bilayers would be of utmost interest.

### III. Channel-Making Antibiotics

#### A. Gramicidin A

We have seen in Figure 6a the chemical structure of the gramicidin A molecule. A peculiar feature of this natural polypeptide is the fact that its amino terminus (the head) is formylated and that the carbonyl terminus is blocked by an ethanolamine group (the tail). As a result, the polypeptide chain is comprised of 16 peptide linkages with one before the Val 1  $\alpha$ -carbon and one after the Trp 15  $\alpha$ -carbon:



Model building and hard thinking led Urry<sup>41,42</sup> to propose a structure for the conducting dimer. Noting that the alternate L and D succession of the amino acids in the molecule allowed the formation of helical structures with all the side chains pointing toward the exterior and with an alternate up and down orientation of the successive carbonyl bonds, he suggested that each monomer in the dimer adopted the conformation of such a helix, with 6.3 residues per turn, stabilized by 8 CO...HN hydrogen bonds with alternating orientations (Figure 9), and that a junction between the two monomers occurred by head-to-head association involving the formation of 6 hydrogen bonds with the free carbonyl and NH bonds producing a continuous helical backbone about 30 Å long and enclosing a hole of a size sufficient to accommodate the ions known to be conducted by the gramicidin A channel.<sup>42</sup>

This structure, at first essentially based on model building and considerable insight, was made more

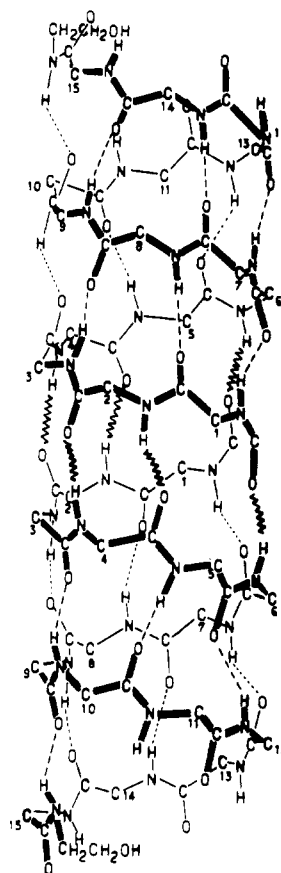
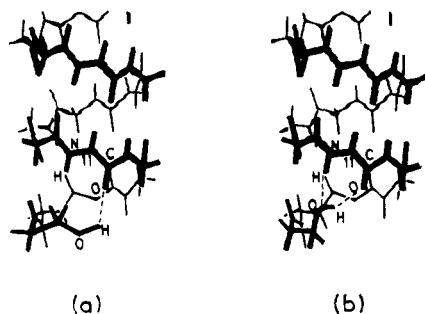


Figure 9. The structure of the backbone in Urry's dimer of gramicidin A (dotted lines and zig-zag lines indicate, respectively, the intra- and intermonomer hydrogen bonds.)

precise by theoretical computations<sup>91</sup> by using energy minimizations with empirical potential functions (cf. also ref 92 for a preliminary account and an interesting discussion). The helical parameters and the  $\phi$  and  $\psi$  torsion angles were determined for left-handed and right-handed  $\beta$ -helices, respectively, and supplemented by a search for the optimal conformations of the side chains, followed by a search for the optimal "docking" of the two monomers into a dimer. Final optimization led to the conclusion of a small preference for the left-handed dimer over the right-handed one by 2.2 kcal/mol. Since then, the structure of the left-handed dimer and the corresponding conformations of the side chains<sup>91</sup> have become known as Urry's structure and are utilized for most theoretical calculations necessitating the atomic coordinates. (Some small differences in the coordinates used by different groups originate from the fact that Urry's coordinates, not published,<sup>91</sup> were reconstituted by using the helix parameters given, but with a slightly different geometry for the peptide unit (cf. ref 93). Other differences have originated in the existence<sup>94</sup> of another set of helix parameters for the backbone, determined by geometrical conditions in a way that is somewhat different from that of Venkatchalam and Urry.<sup>91</sup>)

In the elaboration of Urry's structure, no particular attention was paid to the conformation of the ethanolamine tail of the molecule. It was set,<sup>95</sup> on the basis of model building, as a continuation of the backbone, with its NH hydrogen bonded to the carbonyl oxygen of the Trp 11 residue and with the  $\text{CH}_2\text{CH}_2\text{OH}$  end turned in such a way as to point the hydroxyl oxygen





**Figure 10.** The conformation of the ethanolamine terminal in gramicidin A: (a) in Urry's structure, and (b) after optimization (adapted from ref 108).

toward the exterior of the channel, on the edge of the dimer approximate cylinder. Etchebest and Pullman<sup>96</sup> drew attention to the possible importance of the conformation of the ethanolamine tail and performed an energy optimization of its dihedral angles with respect to the rest of the molecule (optimization done in vacuo, to be consistent with the rest of the structure<sup>91,92</sup>). The results indicated that, in the intrinsically preferred conformation, the hydroxyl group adopts an orientation stabilized by two hydrogen bonds, one involving its oxygen and the NH bond of the Trp 11 residue and the other involving its end hydrogen and the carbonyl oxygen of the same residue (Figure 10). It was observed in calculations of energy profiles<sup>96-98</sup> that the orientation of the ethanolamine terminal influences the location of the energy minimum at the entrance of the channel and, as a consequence, its interpretation in terms of the "binding site".<sup>99</sup> This stressed the possible importance of flexibility of the ethanolamine terminal upon passage of the ion.

Urry's left-handed structure, with the optimized conformation of the ethanolamine tail, is given in Figure 11. A notable feature of the proposed conformation is the orientation of the tryptophan side chains. Trp 9 and 15 are stacked and clustered on one side of the dimer, while Trp 11 and 13 occupy different positions with different orientations on the other side. Although these orientations of the tryptophans have been accepted throughout the years as an integral part of the structure, it must be kept in mind that they correspond to optimizations in vacuo (which in fact yielded a number of possibilities with little differences in stabilities) and that there exists no experimental proof that the above conformations are those prevalent at the contact with the lipids in the membrane. We shall come back to this and other structural puzzles (see ref 100) later.

The availability of a structure at atomic resolution, even though largely hypothetical, opened the possibility for theoretical calculations on the entire gramicidin A dimer, thus permitting, most particularly, explicit evaluation of the influence of the channel's different molecular constituents on the "energy profile" felt by an ion crossing it. Early considerations on energy profiles did not attempt to evaluate the relative depths and heights of the minima and maxima admittedly created by the structure of the walls.<sup>101a,b</sup> The first explicit introduction of this structure used a set of dipoles disposed on a cylinder<sup>102a-c</sup> to represent the carbonyl groups. This simple representation associated with the use of oscillating dipoles allows relatively easily

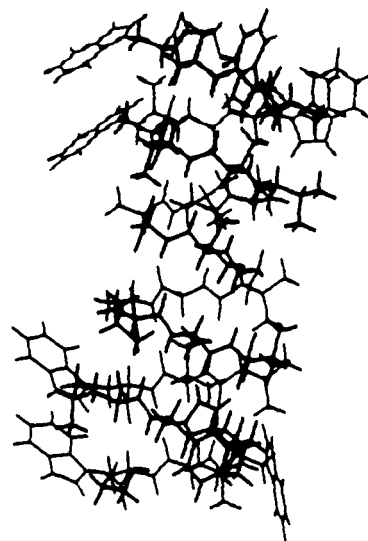


**Figure 11.** Schematic view of Urry's left-handed dimer (with the optimal conformation of the ethanolamine tail).

the carrying out of molecular dynamics calculations.<sup>102b,c,103</sup> It has been utilized extensively<sup>104a</sup> (see also ref 105) even up to recent time with progressive inclusion of structural refinements such as the introduction of NH dipoles and the utilization of the backbone coordinates to locate the center of mass of the dipoles. The model has the advantage to reduce considerably the dimensions of the gramicidin system (otherwise a 552 atoms problem), thereby allowing not only the consideration of the dynamics of the channel wall but also the inclusion of water molecules nearly ad libitum especially if a simple polarizable electropole model is utilized.<sup>104a,c-e</sup>

Owing to their very nature, truncated models can entail artifacts which may be difficult to detect. For this reason, all-atoms calculations<sup>106-112</sup> were carried out in a stepwise fashion with the establishment of the intrinsic role envisioned: first each structural element of the gramicidin dimer in the energy profile of the ions, and then the modifications due to water as well as further effects like those due to the flexibility of the structure. An advantage of all-atoms calculations is the explicit inclusion of the side chains whose role in the channel properties is becoming increasingly apparent (e.g. 113a-d, 114a-d).

### 1. Energy Profiles

In the stepwise all-atom calculations the energy profiles generated by the molecular structure of the dimer were initially evaluated in vacuo, introducing first the backbone only,<sup>106</sup> then the ethanolamine ends,<sup>96,107</sup> and then the side chains.<sup>108</sup> The effect of water was considered in a second stage<sup>97,98,109,110</sup> after determination of the distribution of water alone bound to the dimer. The energy profile was defined as the variation, upon the progression of the ion, of the global energy of the system, ion-dimer for calculations in vacuo, and ion-dimer-water for calculations including water molecules. The ion, placed in successive planes closely spaced perpendicular to the helical axis, was allowed to find its optimal position in each plane by energy minimization (cf. refs 56, 65, and 99 and references cited therein). The same procedure was used in the presence

of water, allowing then the ion and all water molecules to reoptimize their positions at each step. Except for the ethanolamine terminals, the structure of the dimer was kept rigid. Profiles in vacuo were obtained for  $\text{Na}^+$ ,  $\text{K}^+$ , and  $\text{Cs}^+$ , and profiles in water, for  $\text{Na}^+$  and  $\text{Cs}^+$ . A hypothetical profile was computed in the same way for the nonpermeant calcium ion.<sup>111</sup>

Despite their relative simplicity, these calculations established a few fundamental characteristics, the essential of which are as follows:

(a) The introduction of all the components of the theory of intermolecular forces, in particular (owing to the strong polarizing effect of a cation) the polarization energy<sup>93,99</sup> (a component neglected in most early force fields) is important. This term increases appreciably upon progression of the ion toward the center of the dimer, a consequence of the increasing number of polarizable groups surrounding it, thereby deepening the profile with respect to that resulting from the pure Coulomb component of the energy. The interplay of the different energy components differs according to the size of the ion and leads to a different relative disposition of the energy profiles in the different parts of the channel: for larger ions, e.g.  $\text{Cs}^+$ , the attractive dispersion energy manifests itself essentially in the center of the channel<sup>107</sup> where the large size of the ion allows it to interact simultaneously with more atoms than does a smaller ion like  $\text{Na}^+$ , hence providing more attractive terms and thereby lowering the central barrier (see refs 104a,c, 117, 118a for similar observations). As a consequence the heights of the energy profiles in vacuo are in the order  $\text{Cs}^+ < \text{K}^+ < \text{Na}^+$  in the central region while the reverse ordering occurs in the early part of the channel, where the electrostatic component dominates the interactions. The importance of a proper relative location of the profiles appears in the comparison of the relative heights of the entrance and/or central barriers for different ions (cf. point g, below).

(b) Allowing the ion at each step to optimize its position permits its optimal approach to the attractive centers provided by the successive carbonyl oxygens which line up along the channel wall. As a result, the profile shows successive minima and maxima which follow essentially the distribution of the carbonyls along the wall, particularly that of the L carbonyls which, in Urry's model, are tilted by 18–19° toward the interior, whereas the D carbonyls are inclined by 15–16° toward the exterior to ensure the best appropriate array of  $\text{CO}\cdots\text{HN}$  hydrogen bonds. Owing, however, to the presence of all the other atoms, to the simultaneous attraction of different carbonyls and to the delicate balance of the different terms in the total energy at the most stable positions, the minima in the profile do not necessarily face a carbonyl and neither do the intermediate local barriers face the intermediate atoms of the polypeptide chain. The depth of the local minima is more conspicuous for relatively small ions like  $\text{Na}^+$ , much less for large ones like  $\text{Cs}^+$  which can interact with more than one carbonyl at a time.<sup>109</sup> Profiles calculated for an ion constrained to remain on the axis of the channel are smooth curves that lack the details of the minima and barriers and, thus, can be misleading.

(c) The global effect of the side chains on the profiles produces an overall deepening of the energy with respect to that computed without them, the largest effect

being observed near the channel entrance.<sup>108</sup> This can be assigned to the favorable electrostatic contribution due to Trp 13 and 11 in the early part of the profile, where Trp 9 and 15 give a small repulsive contribution. This was related<sup>108</sup> to the respective orientations of the corresponding tryptophans in the conformation associated with Urry's dimer, noting that in this conformation the dipole moments of Trp 9 and 15 are oriented with their positive ends toward the mouth of the channel, while Trp 11 and 13 have an essentially opposite orientation, a situation producing opposite ion-dipole interactions for the two couples. These observations support the hypothesis<sup>113a</sup> (see also ref 113b,c) that the differences in conductance found upon substitution of the natural side chains of gramicidin A by others could be related to changes in the dipole moments of the substituted amino acids. Recent studies<sup>114a-d</sup> of a series of gramicidin A analogues, inspired by this concept, confirm the fact that the side chains influence the energy profile, and stress the role of their dipole moment and of its orientation. This led to the challenging suggestion<sup>114a</sup> that the orientation of the tryptophans in gramicidin itself may be different from that generally assumed and such as to maximize its overall polarity. It will be interesting, in this connection, to have a confirmation of a preliminary announcement<sup>113d</sup> of the results of biased Monte Carlo and high-temperature molecular dynamics calculations on the tryptophan orientations in gramicidin A. It may be expected that the direct interaction of the side chains with the lipids may alter conformations of these chains. Only preliminary results are available on this subject.<sup>114e</sup>

(d) The relative heights of the intrinsic profiles obtained for the alkali ions can be analyzed<sup>107</sup> to indicate the relative heights of the entrance barrier for the different ions, approximating the barrier by the energy balance between the binding energy at the beginning of the channel and the (experimental) dehydration energy of the ion. The order of the resulting values,  $\text{Cs}^+ < \text{K}^+ < \text{Na}^+$ , as well as the relative order of the central barriers, are in agreement with the selectivity preference  $\text{Cs}^+ > \text{K}^+ > \text{Na}^+$  of gramicidin A and with the relative heights of the barriers deduced from rate-theoretical interpretations of conductance data<sup>115,116</sup> (see point g, below).

(e) The reasons for the nontransport of divalent cations can be understood on the basis of their computed profiles.<sup>111</sup> The energy of binding of  $\text{Ca}^{2+}$  is very favorable but its desolvation energy is so high as to make the balance very unfavorable, thus the entrance very unlikely. Furthermore, should the ion succeed to enter the channel, the calculated profile inside shows that the depth of the energy minima and the resulting height of the central barrier would make the transit unlikely.

(f) An interesting attempt to model the effect of a second ion on the profile of the first one<sup>106</sup> showed that it results in a lowering of the central barrier and a facilitation of the exit. An alternative computation involving a truncated model, but including water,<sup>104b</sup> confirms this conclusion.

(g) Comparison of the profiles obtained for  $\text{Na}^+$ <sup>97,98</sup> and  $\text{Cs}^+$ <sup>106</sup> in the absence of water and in its presence shows the interplay of the intrinsic attraction of the channel for the ion and of the progressive loss of ion-



water interactions upon entrance, which results in an appreciable entrance barrier higher for  $\text{Na}^+$  than  $\text{Cs}^+$ , preceded by a wide external energy minimum. Similar results were obtained in molecular dynamics calculations<sup>117,118a</sup> (see also ref 104a,c).

(h) The analysis of the energy profiles in water led to an interpretation<sup>99</sup> of the relation between the calculated profile and the location of the "binding site" deduced from NMR measurements of  $^{13}\text{C}$  chemical shifts of each individually labeled carbonyl carbons of the molecule: these shifts lead to the localization of<sup>119</sup> the "binding site" between Trp 11 and 13, in the neighborhood of Trp 11. It was shown by calculation<sup>97,99,110</sup> that the ion remains in close interaction with the carbonyl oxygen of Trp 13 in the first part of the wide minimum preceding the entrance barrier, and then with that of Trp 11 in the second part of this minimum and all along the entrance barrier. This points to a large probability of residence of the ion in the corresponding zone. All along the entrance barrier, the ion is in contact with the carbonyl of Trp 11 and each unsuccessful attempt to overcome the barrier brings it back to the preceding energy well, hence a longer residential time, thus a larger chemical shift for the  $^{13}\text{C}$  of Trp 11, then of Trp 13. It thus appears that the location of the "binding site" in the phenomenological NMR-deduced profile<sup>120</sup> results from a combination of the relative positions of the energy minimum and of the desolvation barrier immediately following it, which, by keeping the ion in the neighborhood of the carbonyl of Trp 11 for a longer time results in a larger chemical shift. In the profile calculated in vacuo the presence of a deep minimum due to the attraction of the hydroxyl oxygen of the tail at 10.5 Å from the center of the channel has led to its early interpretation, as corresponding to the NMR "binding site". The new interpretation seems more likely. A similar location of the binding site found for  $\text{Cs}^+$ <sup>121</sup> can be interpreted similarly.<sup>109</sup> The analogous location of the "binding sites" for other cations<sup>122a</sup> can probably be related to an analogous behavior linked to desolvation. A preliminary announcement<sup>122b</sup> that the  $\text{Tl}^+$  binding site seems to be appreciably closer to the channel center than expected for monovalent ions would seem, if confirmed, to require a proper theoretical study of the characteristics of Tl binding, taking into consideration the results of recent equilibrium binding NMR studies.<sup>122c-e</sup>

## 2. Water Structure

The distribution of water in the gramicidin A channel without ions has been studied by energy optimization of 16 water molecules added step-by-step<sup>97,98</sup> to Urry's dimer, with the tail in its optimized conformation; by Monte Carlo calculations<sup>123</sup> using Urry's coordinates and introducing 81 water molecules; in an early short (5 ps) molecular dynamics simulation with 13 water molecules,<sup>117</sup> and more recently, in a longer (70 ps) simulation<sup>124</sup> by starting with Koeppe and Kimura's coordinates and including 23 waters. All these calculations found a "single file" of water molecules inside the channel, in agreement with inferences based on various experimental measurements.<sup>125a</sup> While the number of water molecules in the file, deduced from the experiments varies from 6 to 12,<sup>125b,101b</sup> calculations are in better mutual agreement, indicating 7–9 molecules<sup>97</sup>

according to the limits chosen, 8 or 9 in ref 123 and in the early molecular dynamics simulation, 8 in the more recent simulation.<sup>124</sup> The structure of the file presents more differences, while all molecules appear hydrogen bonded to each other in the rigid channel,<sup>97,123</sup> the molecular dynamics calculations find at least one break in the chain. All computations agree on the binding of practically every water to the backbone of gramicidin A, but details differ somewhat, particularly between the frozen and labilized structures. Differences are also seen in the orientations of the water dipoles in the file: whereas the early short simulation led to a structure where all the water dipoles point essentially in the same direction, the longer one indicates an initial "state" with dipoles symmetrically oriented in two files toward the center, a transition to the aligned state occurring after about 30 ps, the authors admitting however that there is "yet no way to judge from the results as to which conformation has the higher free energy".<sup>124</sup> The question of the choice between these two states may be more academic than really important, insofar as the nonrigid character of the file seems well established. The most important feature of the water structure in the channel is the "single-file" structure, which is essentially a result of the narrowness of the space available. For this reason care must obviously be exercised in extrapolating the "file" results to other channels.<sup>126</sup>

## 3. Water and Ions

As a result of the narrowness of the channel, hydrated ions must abandon most of their waters of solvation upon entering the gramicidin dimer: the stepwise desolvation process<sup>97,98</sup> shows the correlation between this process and the shape and height of the entrance barrier (about half for  $\text{Cs}^+$  than for  $\text{Na}^+$ <sup>109</sup>), the profiles in water compared to those in vacuo indicating that desolvation is the major determinant of the entrance barrier. All calculations agree on the fact that the ion, once in the channel, pushes the file of water molecules in front of it while a new file reforms at its back.<sup>97,98,117,118a,123,127</sup> Details of the reorientations of the water molecules differ, however, according to authors and procedure (see ref 104a). The number of water molecules in the file is influenced by the size of the ion, large ions taking up more space.<sup>109,117,118a,b</sup> The presence of water inside the channel appreciably dampens the interaction of the ion with the ligands, thereby affecting the location of the deepest minimum<sup>97,98,109</sup> (see also 127, 104a). (Note that this effect can be appreciated only by comparison of calculations in water and in vacuo, pointing again to the utility of proceeding stepwise.)

The numerical values of the barriers to ion translocation deduced from the experimental rate and binding constants are not satisfactorily reproduced in any of the computations quoted above, whatever the sophistication introduced, suggesting the necessity to introduce the polarization of lipids and the effect of bulk water.<sup>104a</sup> A recent computation of the free energy profile for  $\text{Na}^+$  introducing these effects in a gramicidin dimer (devoid of the side chains) by using the protein dipoles Langevin dipole (PDL) methodology and also a more elaborate (electrostatic) free energy perturbation method with molecular dynamics, has led to  $\delta(\Delta G)$  values of about 5 kcal/mol<sup>128</sup> between the solvation free energy of  $\text{Na}^+$  in the outside bulk solvent and that in the interior of

the channel, a more satisfactory order of magnitude, an encouraging agreement indeed. The question of the central versus entrance barrier, an apparently important issue in the understanding of the conductance behavior (cf. for instance, ref 114a), was not considered.

#### 4. Flexibility and Librations

The question of the flexibility of the channel was raised quite early.<sup>92</sup> To explain the surprising observation that the rate of entry of a second ion in the channel is higher than the rate of entry of the first ion, it was suggested that the entry of the first ion induces a conformational change of the structure, involving a correlated "libration" of all peptide planes, and energy calculations, involving such correlated librations while maintaining the helical parameters indicated the feasibility of such a process.<sup>129</sup> The reality of the phenomenon was questioned in a more recent analysis of the normal modes of the gramicidin dimer,<sup>130</sup> where it was found that the motions of the amide planes were correlated only with those of their nearest neighbors in space rather than with all others. The calculations show, however, a large flexibility of the structure, indicative of the possibilities of deformations along the passage of an ion. The 70-ps molecular dynamics computations without ion<sup>124</sup> indicate an intrinsic tendency of all carbonyls to bend toward the interior of the pore, and also variable deflections of the NH bonds toward the exterior in apparent fair agreement with very recent NMR indications<sup>131a</sup> (cf. however ref 131b). The average bending of the carbonyls was found<sup>118a</sup> to be accentuated by ions, especially the small ones, a larger deflection being apparent at the dimer junction, a result of the near costless deformability in that region. A mention must be made in this connection of a recent<sup>132</sup> interesting discussion of the possibility that the deformability of the pore can facilitate the (otherwise impossible) transit of large weakly permeant organic ions through the dimer.

#### 5. Helix Handedness

The latest structural problem facing both experimentalists and theorists in the domain of the conducting dimer is that of the handedness of the  $\beta$ -helix. The problem was raised by the conclusions of 2D NMR measurements on gramicidin A in dodecyl sulfate micelles,<sup>100,134</sup> which indicated a structure "resembling that of Urry's dimer except for the handedness of the helix".<sup>100</sup> In fact, a detailed examination of the two structures has pointed out<sup>133</sup> that they differ by much more than the handedness of the helix: aside from the fact that the directions of the L and D carbonyls are inverted in the micellar structure with respect to Urry's one, the location of the carbonyl oxygens with respect to the center of the channel is different due to the inversion of the peptide bond directions: from the mouth toward the center in the first monomer, the order is 15, 13, 11, 14, 9, 12, 7, 10, 5, 8, 3, 6, 1, 4, 2, formyl, whereas in Urry's dimer it is 14, 12, 15, 10, 13, 8, 11, 6, 9, 4, 7, 2, 5, formyl, 3, 1, in Arseniev's et al. structure. While, in Urry's model, the carbonyls of the L and D residues point regularly alternately inside and outside, the micellar structure is irregular with the carbonyls of residues 15, 13, 11, 8, 7, 6, 4, and 3 turned inside. Furthermore the NH bond of the ethanolamine moiety

points toward the aqueous phase in the micellar structure, but toward the center of the channel in Urry's dimer. Last, but not least, the orientations of the side chains, particularly those of the tryptophans, are appreciably different in the two structures. Aside from the fact that no stacking is seen between Trp 15 and 9 in the new structure, Trp 13 and 11 have an orientation inverted relative to that of the "standard" dimer. As a result the dipole moments of all the tryptophans in one monomer point essentially in the same direction.

Reoptimization of the two structures<sup>133</sup> under the same conditions, although modifying individually all the atomic positions, does not alter the essential differences listed above. Concerning the difference in energy between the two optimized structures in vacuo, it is only 8 kcal/mol in regard to a total of about 400 kcal/mol in spite of all the structural differences observed, and the gap vanishes completely when a distance-dependent dielectric constant is used. Clearly the two forms have very similar intrinsic stabilities.

In the hope of helping to decide between the two structures, the energy profiles which they generate for  $\text{Na}^+$  were computed both in the optimized structures, maintaining rigidity, and by allowing the entire structure to reoptimize upon progression of the ion.<sup>133</sup> A great similarity was found in the shape of the profiles for the two structures (the modifications due to optimization are important but similar for the two structures) but these analogous profiles cover quite different underlying features, in particular, they concern the residues in close interaction with the ion in the deepest energy minima. In the libalized micellar structure, the carbonyls in close contact with  $\text{Na}^+$  comprise Val 8 but not Leu 14, while in the libalized Urry's dimer, Leu 14 is involved but not Val 8. This, in conjunction with the observation of a  $^{13}\text{C}$  chemical shift for Leu 14 but not for Val 8, would favor the left-handed structure for the channel form, a confirmation of an early inference by Urry et al.<sup>135</sup> It remains, however, to be seen whether the introduction of water in the two structures would not modify these conclusions especially in view of the latest experimental evidence (on gramicidin A in DMPC bilayers) concluding definitely to a right-handed sense of the helix<sup>131b</sup> (cf. also the recent indications of hybrid-channel experiments.<sup>131c</sup>)

#### 6. Other Structures

An important issue, at least until recently, has been the controversy between the tenants of Urry's head-to-head  $\beta$ -helical structure and those of a double-helical configuration<sup>136a</sup> for the channel form of the gramicidin dimer. Although the controversy seems to be settled in favor of Urry's structure, probably right-handed, (vide supra) for the membrane-bound channel form, double-stranded helical structures seem to prevail in solutions.<sup>136b</sup> One such form was characterized in the cesium chloride crystal,<sup>136c</sup> and another more elongated one in an ion-free crystal.<sup>136d</sup> The proposal<sup>136e</sup> that double helices may act as ion channels was investigated by calculations<sup>136f</sup> of energy profiles (using backbone coordinates<sup>94</sup>) which concluded that such a form should be cation selective but less capable than Urry's dimer to transfer ions.

The mechanism of ion inclusion into the double helix and the interconversion of the different forms are in-

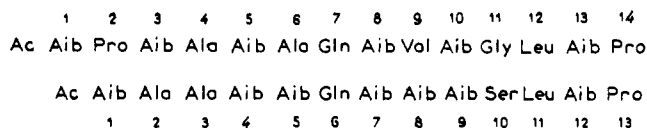


**Figure 12.** The correspondence between the N-terminal segments of the sequences in alamethicin IA and trichlorzianine TIIIc.

interesting theoretical problems yet unsolved.

In summary, even if a number of problems remain which have hardly been touched (such as, in particular, the exact role of long-range electrostatic forces in the modeling of ion pores in membranes<sup>128,136g</sup>) the calculations on gramicidin A have taught us a number of lessons concerning the structure–function relationship in channels: some have a general character, others apply only to the molecule concerned. In the first lot are the importance of all energy components and the differences in their respective weights in different regions and for different ions, the necessity of letting the ion optimize its position, the determinant role of the carbonyl oxygens lining the inner wall in providing a favorable “solvation” of the ion inside the channel, the role of all the structural constituents of the channel, and the importance of examining the structure-related path of the ions underlying the overall profile. The distribution of water inside the channel and the considerable role of the desolvation process to the point that the ion abandons all but two of its water molecules upon entry, largely as a result of the relative narrowness of the pore, may or may not be relevant to other channels.

## B. Alamethicin and Macrolide Channels

While alamethicin and its analogues have been the object of a considerable number of experimental investigations, very little work using the methods of theoretical chemistry has been carried out on these molecules and their channel properties. Notable is a recent effort<sup>137</sup> toward a comparison of the conformational and aggregation properties of alamethicin and of one of its analogues trichorzianine, inspired by some of the hypotheses made in building models<sup>43–45</sup> of the alamethicin channel. In these models a special role is ascribed to the 14 amino acid  $\alpha$ -helical segment of the N-terminus of the molecule (up to Pro 14) which is assumed to insert into the membrane where it forms aggregates, admittedly transformed later into bilayer-spanning bundles enclosing a channel. In the model, based on the crystal structure of alamethicin,<sup>43</sup> the side-chains of the glutamine residues in the seventh position of neighbor  $\alpha$ -helices are assumed to favor the packing by forming an array of hydrogen bonds between their amide groups. The analogue trichorzianine presents a number of similarities and differences with the parent compound (Figure 12). Theoretical calculations concentrated on the N-terminal portion of the two molecules, up to Pro 14 in alamethicin, and up to Pro 13 in trichlorzianine, in view of a comparison of their helical character and of their aggregation properties, with a particular emphasis on the possible role of the glutamine residue. Complete energy optimization indicated that the Ac...Pro 13 segment of trichlorzianine is essentially  $\alpha$ -helical with a bend starting three residues before the proline, a structure quite comparable to that found for the Ac...Pro 14 corresponding segment

of alamethicin, but comprising furthermore two weak  $n$  to  $n + 3$  hydrogen bonds in the first helical turn, an indication of a slight tendency to a  $3_{10}$  character (cf. ref 137 for a discussion in connection with apparent contradictions concerning the structure of these Aib-containing helices). Calculations of the pairing properties of the respective optimal helices showed that different modes of near-parallel pairings are possible for both molecules, indicating a possible, but not indispensable, intervention of the glutamine residue. The mode of formation of larger aggregates and their transformation into channel-containing bundles were not yet considered.

Macrolides of the amphotericin B-type form complexes with cholesterol and make channels in membranes. Model building<sup>46,47</sup> assumes that the macrolide–cholesterol complexes aggregate in the membrane into cylindrical half-pores which then associate to form a continuous aqueous channel. The interactions involved have only recently started to interest theoreticians. Mention must be made of an early calculation of the conformational properties of amphotericin B which concluded to an overall rigidity of the macrocycle.<sup>138</sup> The complexation with cholesterol was considered recently with emphasis on the conformation of the polar head of the antibiotic in vacuo and in water,<sup>139</sup> concluding to the possibility of the intervention of a bridging water molecule in the macrolide–sterol complex. A more extensive study<sup>140</sup> of the complex led to two stable states, which were used to model open and closed channels. Channel–water–chloride ion systems investigated by Monte Carlo computations point to the role of dehydration upon ion entrance.<sup>141</sup>

## IV. Ion Channels in Membrane Proteins

### A. Bundles of Hydrophobic $\alpha$ -Helices

An early model of the proton pump bacteriorhodopsin, based on low-resolution maps of electron-scattering density,<sup>24</sup> described the membrane-spanning portion of the protein as made of seven rods attributed to  $\alpha$ -helical hydrophobic segments of the polypeptide chain crossing the bilayer perpendicularly to the surface and closely packed together on the edges of a distorted heptagonal prism, a structure very recently confirmed by refinement at near-atomic resolution.<sup>25</sup> The detection of “hydrophobic segments” of 20–30 amino acids by sequence analysis of numerous membrane proteins, (cf. refs 142–146a) and further model building encouraged the generalization of the concept that *ion channels in membrane proteins are formed within bundles of hydrophobic  $\alpha$ -helices*. In parallel, the consideration of channel formers like alamethicin and the observations that synthetic hydrophobic polypeptides showed channel behavior in bilayers was also interpreted in terms of their formation of helix bundles.<sup>146b–f</sup> The basic idea that hydrophobic polypeptide segments cross membranes as  $\alpha$ -helices has received experimental support from the detection of such helices in the crystal structure of the photosynthetic reaction center<sup>22,23</sup> and also now of bacteriorhodopsin.<sup>25</sup> Concerning the rest of the “bundle hypothesis” given above, it was observed<sup>147</sup> that the essential existing knowledge on the structure, folding, and interactions derived experimentally and theoretically from the consideration of

soluble proteins was unlikely to be transferable to the problems concerning the packing properties of hydrophobic  $\alpha$ -helices of the appropriate lengths in membranes or their aptitude to form bundles enclosing channels capable of binding and/or transport ions. A systematic theoretical study was therefore undertaken by using energy optimization procedures (cf. refs 65 and 99 and references cited therein) to address in particular the following questions:

How do hydrophobic  $\alpha$ -helices aggregate?

Can they form stable bundles?

Which component(s) of the energy govern the aggregation?

Are these bundles apt to form channels, that is, can a stable aggregate enclose a hole appropriate for an ion to pass?

Can an ion be accommodated and transported in a pure hydrophobic channel, or must the inner wall be lined by polar and/or charged amino acids?

How can the opening and closing of channels in bundles be envisaged?

Consideration of the pairing properties of hydrophobic  $\alpha$ -helices of different length and composition,<sup>148,149</sup> of the structure and stability of bundles of such helices as a function of their number and amino acid content,<sup>149-151a</sup> and of the aptitude of a pore enclosed within a bundle to accommodate and transfer a cation and/or water<sup>149-151b</sup> has led to interesting conclusions.

### 1. Pairing Properties of Hydrophobic Helices of Increasing Length

The key element governing the aggregation of hydrophobic  $\alpha$ -helices is contained in their pairing properties. This was put into evidence by considering the effect of the length of hydrophobic  $\alpha$ -helices on the energy and conformational characteristics of their most stable pairs. It was found<sup>148,149</sup> that: (i) in the optimal pairs of two (L-Ala)<sub>n</sub> chains the two helices are nearly antiparallel and closely aggregated in a mode which is akin, but not identical, to the "knobs into holes" mode, the structure of the pair becoming constant beyond the length corresponding to  $n = 13$ , (ii) the interaction energy of the two helices increases regularly with  $n$ , (iii) the electrostatic and van der Waals/London components of this energy contribute both to the stability of the pairs, but while the electrostatic component tends toward an asymptote, the London attraction increases continually with the number of residues, hence dominates the energy (after  $n = 13$ ) (Figure 13). The generality of these results was confirmed<sup>151a</sup> upon substitution of alanines, on the faces of contact of the helices, by bulky side chains, namely leucines.

The fact that the van der Waals/London energy is negative (favorable) and increases with  $n$  is a reflection of the hydrophobic nature of the groups in interaction which give rise to an attractive dispersion energy dominating over the repulsion term, an effect which increases with the number of these groups at the interface and also with their bulkiness.<sup>151a</sup>

The fact that the electrostatic component of the interaction energy reaches an asymptote relatively rapidly is sometimes considered surprising on the basis of reasoning on dipole-dipole interaction of helices but it must be kept in mind that whereas it is true that the

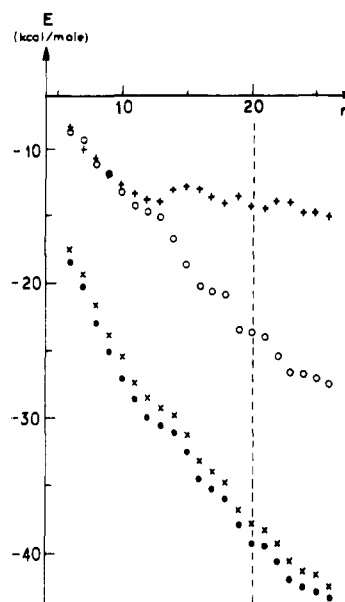


**Figure 13.** Evolution of the energy and of its components in the optimal antiparallel pairs of (L-Ala)<sub>n</sub> for  $n = 6-26$ : (●) total energy, (×) total minus polarization energy, (+) electrostatic component; (○) repulsion + dispersion component. The vertical line at  $n = 20$  indicates the minimal number of residues necessary to span the lipid phase of the membrane (adapted from ref 148).

dipole moment of an  $\alpha$ -helix increases regularly with the number of peptide bonds,<sup>153</sup> this does not imply (as often hastily concluded) that the interaction of the two helical dipoles increases in the same way.<sup>148-151b</sup>

This behavior of the two main components of the binding energy of a pair has far-reaching implications for the aggregation properties of hydrophobic polypeptidic segments in membranes: in order to span the 30-Å width of the lipid part of a bilayer, the  $\alpha$ -helices must contain at least 20 residues. At this length, the electrostatic term has largely reached its asymptote and the van der Waals/London component dominates the energy, thus the aggregation. This dominance is particularly strong in the real membrane proteins where the hydrophobic segments contain a large number of bulky hydrocarbon groups like leucines, isoleucines, valines, phenylalanines, etc. This indicates that the hydrophobicity of the transmembrane segments of membrane proteins serves not only to insure a favorable interaction with the surrounding lipids but also to insure favorable lateral interactions between the helices, thereby favoring bundle formation.

Another consequence of the dominance of the dispersion term over the electrostatic component of the energy is the possibility of existence of stable parallel pairs. Indeed explicit calculations for helices of more than 13 residues showed<sup>137,149,151a</sup> that optimized parallel pairs of sufficient length can be stable: in that case the electrostatic interaction is unfavorable as expected for the interaction of two nearly parallel dipoles, but the repulsion/dispersion energy (dominated by the favorable dispersion term) overcompensates the electrostatic term, leading to a stable structure. This conclusion is strengthened if the presence of the lipid surrounding milieu is taken into account by introducing a dielectric constant, since, whatever the value of this constant, its effect is to decrease even further the relative weight of the electrostatic component in the total energy of interaction.

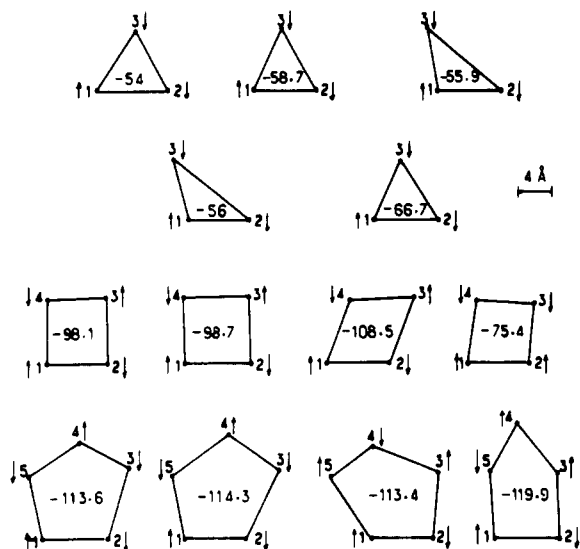


**Figure 14.** Schematic view (from the C-terminus of h1) of the shape of stable bundles of  $N$  (L-Ala) $_{14}$  for different values of  $N$ . Energies in kilocalories per mole (adapted from ref 149).

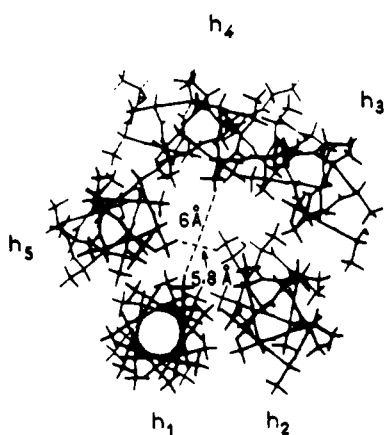


**Figure 15.** The hole in a bundle of five (L-Ala) $_{14}$ .

## 2. Bundles of $N$ Hydrophobic $\alpha$ -Helices

By taking advantage of the previous results, the formation of bundles was examined by energy optimization of packages of  $N$   $\alpha$ -helices of (L-Ala) $_{14}$  for  $N = 3-7$ . For each  $N$ , the helices were initially disposed along the edges of polygonal prisms of different shapes and alternately oriented up and down (to possibly represent the threading of the membrane  $N$  times by a single polypeptidic chain as in bacteriorhodopsin). Energy optimization, allowing  $N - 1$  helices to use their six degrees of freedom with respect to one kept fixed, showed that:<sup>149</sup>

(i) For each  $N$ , a number of stable bundles can be found with different shapes and very similar stabilities (cf. Figure 14).

(ii) For  $N$  sufficiently large, the bundles can enclose a hole of sufficient size to provide a channel (cf. Figure 15 for an example).

(iii) As shown by the strong negative values of the energies, all the structures are very stable including those which contain pairs of adjacent parallel helices. (Note the case of two such pairs in a quadrangle.)

The validity of these conclusions for hydrophobic segments containing more bulky side chains (such as those observed in membrane proteins) was tested by

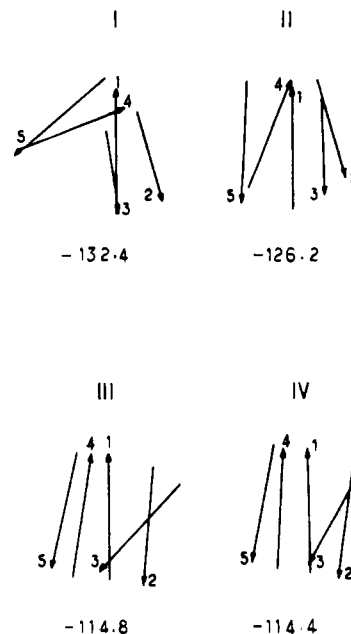


**Figure 16.** The relative positions and orientations of the helices in four stable bundles of five segments containing interfacial leucines. Energies are in kcal/mol. Arrows go from the N-terminus to the C-terminus (adapted from ref 151a).

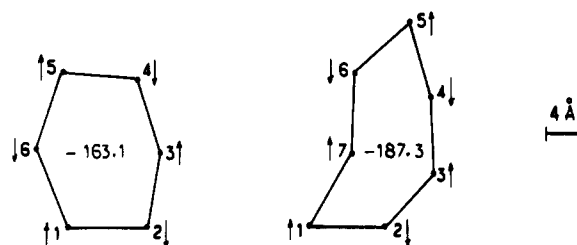


**Figure 17.** The bundles of six and seven (L-Ala) $_{14}$  optimized by starting from a regular polygonal prism (adapted from ref 149).

considering the effect of the presence of leucines on the faces of contact between the helices on the packing as well as on the shape and properties of bundles, starting with a number of initial pentagonal prisms (cf. ref 151a for details). It was observed that the bulky interfacial side chains make the rotations of the helices around their axis more difficult than when they contain alanines only, so that, aside from sliding, the major conformational adjustments of the helices are their relative inclinations (cf. Figure 16). As a result, the hole enclosed within the bundles varies in dimension and shape (from conical and irregular to more cylindrical and more regular). These observations showed explicitly, for the first time, *how a modulation of the size and shape of a channel can be associated with the tilting and/or sliding of the helices, providing a basis for the concept of the opening/closing of a pore via conformational changes* like those which have been envisaged, for instance, in the nicotinic acetylcholine receptor protein (cf. for instance ref 154).

(iv) When the number  $N$  of helices is large, the search for the most stable aggregate leads to a final shape that is quite distorted with respect to a regular polygonal prism, even when starting with this regular structure (cf. Figure 17). This result comes from the fact that the helices tend to adopt a structure insuring the largest possible number of close pair interactions. (Note in particular the shape of the heptamer structure, remi-

niscient of the shape of the seven helix bundle which exists in bacteriorhodopsin,<sup>25</sup> a possible indication that, aside from the constraints imposed by the composition of the helices in this molecule, the observed packing may reflect a tendency to an optimal arrangement.)

### 3. The Capacity of a Purely Hydrophobic Bundle To Act as an Ion Channel. Role of Polar Residues

The next question considered was whether it is energetically possible for a cation to be accommodated and transported in the interior of a bundle made of purely hydrophobic helices. With  $\text{Na}^+$  used as a probe in the pore of the pentahelix bundle of Figure 15 to calculate an energy profile,<sup>149</sup> first in the channel that was maintained rigid, and then by allowing the structure to reoptimize upon passage of the ion, it was found that:

(i) *The interaction energy of  $\text{Na}^+$  with the bundle is favorable everywhere, despite the presence, on the inner walls of the pore, of the protruding methyl groups and the absence of polar and/or charged side chains, the elements responsible for this situation being the stabilizing interactions between the ion and the peptide carbonyl oxygens on the walls. Although it could have been inferred from the gramicidin case, the role of the carbonyls on the channel walls was not appreciated before the theoretical calculations. Attention was rather centered on the unfavorable effects of the internal hydrophobic side chains (absent in gramicidin).*

(ii) *The labilization of the structure improves the profile, by removing hindrances thus permitting better interactions.*

(iii) *The effect of the presence of polar (nonionized) side chains (studied in a reoptimized bundle including serines on the inner wall<sup>150</sup>) produces an appreciable deepening of the interaction energy, due to the supplementary attraction provided by the hydroxyl oxygens of the serines which take advantage of the flexibility of these side chains to turn, at best, toward the ion. The same was found for glutamine<sup>137,157</sup> and threonine<sup>156,157</sup> side chains. Overall, the attractive character of the end groups of polar side chains, together with the flexibility of their hydrocarbon chain, can help the transit of the ion, either directly or through water molecules.<sup>150</sup> The demonstration of the particular aptitude of serine side chains to play such a role assumed a special importance recently in connection with the role apparently played by such residues in the functioning of the nicotinic acetylcholine receptor channel.<sup>154,155</sup> Needless to say, these results, obtained in computations with partly limited flexibility of the systems and in vacuo, are always open to refinements. It is quite unlikely, however, that their *essence* would be modified although the absolute values of the energies involved would certainly be decreased and thus brought to within a more reasonable range. In fact points i-iii have been entirely confirmed by recent computations.<sup>152a,146e</sup>*

## B. Building of a Model for a Physiological Channel: The Nicotinic Acetylcholine Receptor Channel

In the absence of a three-dimensional structure at atomic resolution of a membrane protein, model building aided by energy calculations integrating the relevant experimental available data, is a reasonable

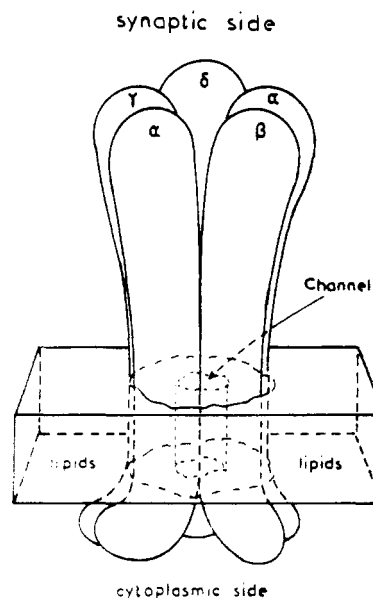


**Figure 18.** Schematic view of the AChR protein crossing the postsynaptic membrane.

way to arrive at a proposal which, then, can be used to possibly help understand, at the molecular level, the functioning of the molecule as an ion channel. Such a model was recently built<sup>156-161</sup> for the channel part of the nicotinic acetylcholine receptor (AChR), by using the presently available structural data together with theoretical calculations and computer-aided molecular modeling as well as the results described in section IV.A. The AChR is particularly appropriate for such modeling because of the considerable amount of structural knowledge available about it. This protein, inserted at the neuromuscular junction in the post-synaptic membrane, acts as a receptor for the neurotransmitter acetylcholine arriving from across the synaptic cleft. The binding of two molecules of the neurotransmitter triggers the opening, within the membrane-inserted protein, of a channel allowing the rapid entry of  $\text{Na}^+$  ions followed by a succession of events leading to muscle contraction.

The basic elements of the receptor structure (for exhaustive source references and an up-to-date discussion of the present state of the experimental evidence see for instance ref 154 and also ref 146a) are the following:

(i) The protein possesses four subunits  $\alpha$ ,  $\beta$ ,  $\gamma$ , and  $\delta$  of known sequences, which are arranged pseudopentagonally, in the stoichiometry  $\alpha^2$ ,  $\beta$ ,  $\gamma$ , and  $\delta$  around a central axis, in the order  $\alpha$ ,  $\beta$ ,  $\alpha$ ,  $\gamma$ , and  $\delta$  as seen from the synaptic side (Figure 18).

(ii) Each subunit possesses four hydrophobic segments MI, MII, MIII, and MIV supposed to cross the membrane as  $\alpha$ -helices.

(iii) The N- and C-termini of the subunits are both on the synaptic side of the postsynaptic membrane, so that, in each subunit, the successive orientations (from the N- to the C-terminus) of the segments MI to MIV are as indicated schematically in Figure 19.

(iv) Converging evidence from conductance measurements on chimeras of different species, affinity labeling experiments with tritiated noncompetitive blockers (NCB), and more recently the probing of the binding site by QX222 in appropriately chosen mutants



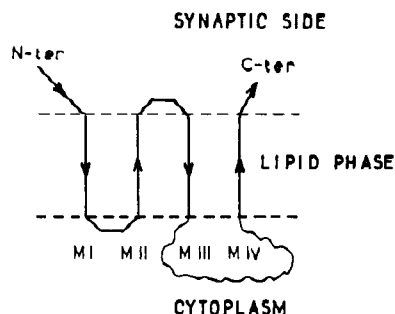


Figure 19. The orientation of the helical segments MI to MIV of each subunit (the packing is not indicated).

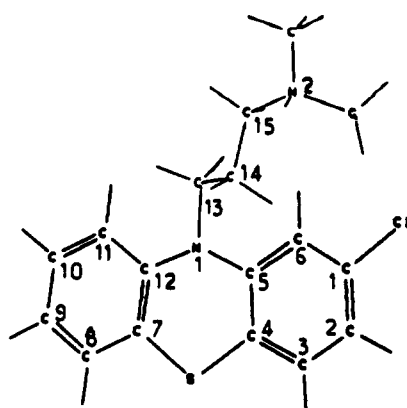


Figure 20. The noncompetitive blocker chlorpromazine.

of the mouse AChR indicate that helix MII of each subunit participates in the inner wall of the channel (cf. ref 154 for a detailed chronological relation of the development of this evidence).

(v) The labeling experiments by the noncompetitive blockers, particularly chlorpromazine (CPZ) (Figure 20), indicated labeling of homologous serine residues on each MII segment, from which two important conclusions were inferred,<sup>155</sup> namely that these serine residues essentially face the center of the pore and that the site of blocking by CPZ is situated at, or near, the level of the labeled serines.

Starting with this premise, a model of the inner wall of the open channel could be developed.

### 1. Shape and Dimensions of the Model

The five MII helices were disposed with pentagonal symmetry around a central axis perpendicular to the membrane, the MII sequences (Figure 21) being aligned in such a way that the labeled serines are at the same level with their  $\alpha$ -carbons pointing toward the central symmetry axis.

The condition that the blocking site of CPZ occurs at the level of the labeled serines was shown<sup>156</sup> to impose that adjacent MII helices are in contact at this level (model A of Figure 22) rather than separated by another helix somewhat behind (as in model B). (It was shown that in model B the axes of two adjacent MII's cannot become smaller than 14.6 Å unless the distance MII-X becomes smaller than 9 Å, a possibility excluded by studies of the pairing of helices with bulky interfacial residues.<sup>151a</sup>)

Adopting therefore model A, the closest possible approach of two adjacent MII's at the level of the labeled serines was determined so that the space enclosed by the five helices is just sufficiently narrow to block the

Synaptic side C terminal of MII			
Ser	Glu	Glu	Glu
Pro265	Pro271	Pro274	Pro279
Ile	Val	Val	Leu
Leu	Lys	Lys	Arg
Glu262	Asp268	Gln271	Gln276
21 Val	Ala	Ala	Ser
20 Ile	Leu	Ile	Thr
19 Val	Leu	Leu	Leu
18 Leu	Leu	Phe	Leu
17 Leu	Leu	Leu	Leu
16 Phe	Phe	Phe	Phe
15 Val	Val	Ile	Val
14 Thr	Thr	Thr	Ala
13 Leu	Val	Gln	Gln
12 Ser	Ala	Ala	Ala
11 Leu	Leu257	Leu	Leu
10 Leu	Leu	Leu	Leu
9 Val	Ala	Val	Val
8 *Ser248	*Ser254	*Ser257	*Ser262
7 Ile	Ile	Ile	Ile
6 Ser	Ser	Ser	Ala
5 Leu	Leu	Leu	Thr
4 Thr	Ser	Thr	Ser
3 Met	Met	Cys	Met
2 Lys242	Lys248	Lys251	Lys256
1 Glu241	Glu247	Gln250	Glu255
Gly	Gly	Gly	Gly
$\alpha$	$\beta$	$\gamma$	$\delta$

Figure 21. The aligned sequences of the MII segments in the  $\alpha$ -,  $\beta$ -,  $\gamma$ -, and  $\delta$ -subunits.

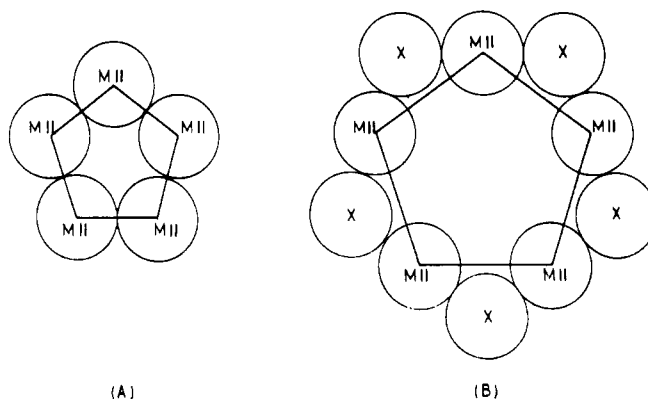
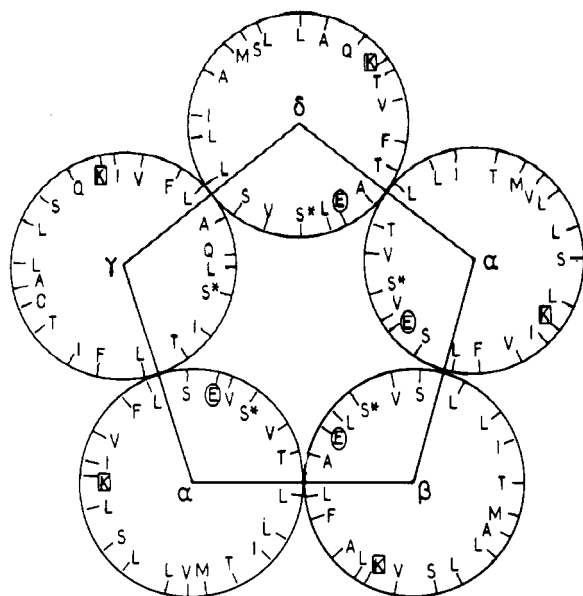


Figure 22. Disposition of the MII segments at the serine level: A blocks chlorpromazine, and B does not.

molecule of chlorpromazine.

Then, the closest possible approach of the helices in the upper region of the channel was determined so that the molecule of chlorpromazine can diffuse freely to its blocking site through the channel without hindrance due to the presence of bulky side chains in this region (Figure 21). Calculation of the minimal diameter of the pore necessary to avoid this hindrance showed<sup>157</sup> that, within the hypotheses adopted, this can best be achieved by a tilt of the five MII helices away from the central axis by about 7°, leaving only a small gap which can be easily blocked by another helix of the bundle.<sup>158,159</sup> The distances of the axes of adjacent MII's in the resulting truncated conical structure is 11.5 Å at the serine level and 14.2 Å at the level of the  $\alpha$ -carbons



**Figure 23.** The helical wheels of the C $\alpha$  carbons (standard one letter convention for amino acids). The starred residues are the labeled serines. The oval denotes the Glu (Gln) residues, the rectangle the Lys residues (see text).

of the extreme upper residues (vide infra).

## 2. The Limits of the Helices and the Role of the Charged Residues

The determination of the hydrophobic segments in the sequence of proteins leaves always a latitude for the assignment of their ends, thus the assignment of the ends of the  $\alpha$ -helices inserted in the membrane.<sup>162,163</sup> In the AChR the presence of polar residues near the extremities of the MII segments complicates the situation further, the tendency being to exclude such residues from the lipid phase, thus from the helices.<sup>163</sup> For building the model the following choices were made:

(i) At the upper end, the helices were terminated four residues below the conserved proline, at Val, Ala, Ala, and Ser, in  $\alpha$ ,  $\beta$ ,  $\gamma$ , and  $\delta$ , respectively, thus excluding from the helical stretch the polar residues which follow.

(ii) At the bottom part of the MII's, the polar residues Glu (Gln in  $\gamma$ ) and Lys preceding the sulfur-containing residues in each MII were, on the contrary, included in the helices on the basis of explicit calculations of energy profiles for the largest permeant ion dimethyl bis(hydroxyethyl)ammonium<sup>156</sup> and also for sodium.<sup>158</sup> These calculations indicated that the exit of the ion was hindered by a considerable energy barrier in a model built with helices excluding the two polar residues, but that this barrier was totally removed upon introduction of these residues in the helical structure. This favorable effect is a result of the favorable location of the five negative residues imposed by the  $\alpha$ -helical structure when the labeled serines face the center of the channel. In such a case the Glu (Gln in  $\gamma$ ) residues are also oriented toward the inside, whereas the positive lysines are oriented toward the helix exterior, and thus do not counteract the favorable accumulated attraction of the negative residues (Figure 23).

Energy optimizations<sup>157</sup> showed furthermore that these orientations allow the formation of stable salt bridges (hydrogen bonds in  $\gamma$ ) which leave a sufficient opening at the bottom of the channel to allow the

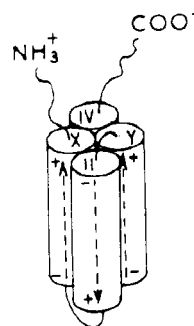


**Figure 24.** Schematic disposition of the four helices in the subunit bundles.

passage of the largest ion transported.

These results pointed to a decisive role, in the transit of the ion, of the negative residues at the N-terminus of the MII segments. A striking confirmation of this conclusion and of the underlying hypotheses of the model was brought about by site-directed mutation experiments<sup>165</sup> on the charged residues in the MII's in AChR and in their neighborhood. It was shown in particular that mutating the negative residues at the bottom level considered above had a much stronger effect on the conductance rather than mutating other negative residues, thus confirming their particular role and also the outside location assumed for the upper negative residues. Also the absence of effect seen upon mutation of the lysines speaks in favor of their location toward the exterior as in the model.

Still more striking confirmations have been brought about by recent calculations of energy profiles in different mutants<sup>160</sup> (see section IV.B.4).

## 3. The Role of the Other Helices

The calculation of energy profiles allows one to go one step further in the refinement of the model.<sup>158</sup> It was observed that, when profiles are calculated in the pentagonal prism of MII helices described above, the interaction energy of the ion with the channel, although favorable everywhere, becomes less and less favorable from the synaptic to the cytoplasmic side, a shape clearly unfavorable to the transfer of a positive ion toward the cytoplasm. An analysis of the components of the energy indicated that it is dominated by the evolution of the electrostatic component, more and more unfavorable toward the channel exit. This can be rationalized by noting that the five nearly parallel helices are oriented in such a way that their strong dipole moments (about 70 D each) with their positive ends at the N-termini add up their effects, disfavoring strongly the transit of a positive ion toward this end. If however, it is remembered that each MII helix is part of a subunit comprising three other helices, the artificial character of the energy result appears immediately. The sequential disposition of the hydrophobic segments in the polypeptide chain of each subunit (Figure 19) and the shortness of the MI-MII and MII-MIII linkers in the amino acid sequences impose that the two segments MI and MIII (which have dipole moments opposed to the MII's) are necessarily close to them in the bundle, somewhat behind, as shown schematically in Figure 24, so that their combined effect will cancel the handicap produced by the dipole moments of the MII's. Indeed the energy profiles, calculated so

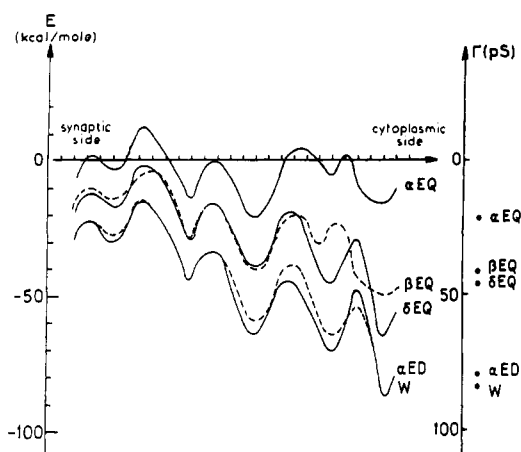


**Figure 25.** Energy profiles for the wild type and four mutants (see text) (adapted from ref 160).

as to take into account this effect, present the appropriate slope for easy transit to occur (cf. ref 159 for technical details). Another recent proposal<sup>152b</sup> for canceling the unfavorable effect of the MII dipole moments invokes the role of partial charges on the cytoplasmic and synaptic terminal residues. This proposal relies on calculations with the PDL algorithm<sup>128</sup> of the energy profile on the axis of a regular pentamer made of five identical MII  $\delta$ -helices comprising 23 residues advocated to be a model of the AChR channel.<sup>152c</sup> Putting, arbitrarily, three negative charges on the ring of five Glu residues, one positive charge on the ring of five lysines, and two positive charges on the ring of arginines, the computed profile compared to that obtained with un-ionized residues shows that the dipole effect has apparently been compensated. It would be desirable to examine the dependence of these results on the distribution of the charges and on the conformation of the arginines in the model adopted (in the Furois-Corbin/Pullman model, based on the real sequence, these arginines are external to the pore).

#### 4. Energy Profiles in Mutants as Confirmation of the Overall Model

Energy profiles were calculated<sup>160</sup> for a sodium ion in the channel, constructed as indicated, for the wild type (nonmutated channel) and for four mutants,<sup>166</sup> those involving respectively the N-terminal glutamates mutated into glutamines in  $\alpha$ ,  $\beta$ , or  $\delta$ , respectively, and into aspartate in  $\alpha$  (notation  $\alpha$ EQ,  $\beta$ EQ,  $\delta$ EQ, and  $\alpha$ ED, respectively). The helices were maintained fixed but the side chains of the internal residues were allowed complete freedom upon ion passage. The striking correlation observed between the average relative location of the energy profiles and the relative values of the conductances measured (Figure 25) is gratifying. Together with the analysis of the structural elements intervening in the ion-channel interaction along the path, shown to allow the understanding of the subtle distinctions between the  $\beta$ EQ and  $\delta$ EQ mutants and even the still more subtle ones between the wild type and the  $\alpha$ ED mutant, this suggests that the overall structural features of the model are essentially correct. The absence of effect seen in mutations of the lysines are another confirmation (see section II.2). In its present stage it appears that the model described incorporates at best the essential available data. Possible

refinements have been indicated.<sup>166</sup>

## V. Concluding Remarks

In the conclusion of this review, it seems appropriate and, we believe, justified to underline the significant contribution of theoretical chemistry to the unraveling of the relatively very complex and diversified mechanisms of ion transport through membranes. This contribution covers three of the main types of transporters involved: ionophores, channel-making antibiotics (the most striking of which is gramicidin A), and a representative of a natural physiological channel, the nicotinic acetylcholine receptor channel. Following the nature of the compounds studied, the complexity of the problems involved, and the relative abundance or lack of experimental data, the theoretical studies alternated between the elucidation of available experimental information (ion selectivity of the ionophores), the determination of the role of the essential components of the molecular structure of channels in the generation of the "energy profiles" (e.g. gramicidin A and the AChR channel), the determination of the basic principles defining the possible formation of channels (e.g. the rules governing the formation of bundles of hydrophobic  $\alpha$ -helices), and the construction of models (e.g. the AChR channel), suggesting further or new experiments. By its ability to study situations in vacuo and in the presence of different media, theoretical chemistry represents a unique tool for the separation of intrinsic and environmental effects in the overall mechanisms of ion transport. In a field where, because of the complexity of the systems involved, both experimentation and theory are difficult, their interplay should be encouraged.

## IV. References

- (1) Alberts, B.; Bray, D.; Lewis, J.; Raff, M.; Roberts, K.; Watson, J. D. *Molecular Biology of the Cell*; Garland Publishing Inc.: New York, 1983.
- (2) *New Comprehensive Biochemistry*; Finean, J. B., Michell, R. H., Eds.; Elsevier: North Holland, Biomedical Press: Amsterdam, 1981; Vol. 1 (*Membrane Structure*).
- (3) Cevc, G.; Marsh, D. *Phospholipid Bilayers. Physical Principles and Models*; Wiley Interscience: New York, 1987.
- (4) Singer, S. J. *Ann. Rev. Biochem.* 1974, 43, 805.
- (5) Khorana, H. G.; Gerber, G. E.; Herlihy, W. C.; Gray, C. P.; Anderegg, R. H.; Nikhei, K.; Biehm, K. *Proc. Natl. Acad. Sci. U.S.A.* 1979, 76, 5046.
- (6) Ovchinnikov, Yu. A.; Abdulaev, N. G.; Feigina, M. Yu.; Kisilev, A. V.; Lobanov, N. A. *FEBS Lett.* 1979, 100, 219.
- (7) Devillers-Théry, A.; Changeux, J. P.; Paroutaud, P.; Strassberg, A. D. *FEBS Lett.* 1979, 104, 99.
- (8) Hunkapiller, M. W. C.; Strader, D.; Hood, L.; Raftery, M. A. *Biochim. Biophys. Res. Commun.* 1979, 91, 164.
- (9) For a review, see for instance: Stroud, R. M.; Finer-Moore, J. *Annu. Rev. Cell Biol.* 1985, 1, 317.
- (10) Schoffield, P. R.; Darlison, M. G.; Fujita, N.; Burt, D. R.; Stephenson, F. A.; Rodriguez, F.; Rhee, L. M.; Ramachandran, J.; Reale, V.; Glencorse, T. A.; Seeburg, P. H.; Barnard, F. A. *Nature* 1987, 328, 221.
- (11) Grenninglow, G.; Rienitz, A.; Schmitt, B.; Methfessel, C.; Zenson, M.; Beyreuther, K.; Gundelfinger, E. D.; Betz, H. *Nature* 1987, 328, 218.
- (12) Olsen, R. W.; Tobin, A. J. *FASEB J.* 1990, 4, 1470 and references therein.
- (13) Numa, S. *Biochem. Soc. Symp.* 1986, 52, 119.
- (14) Caterall, W. A. *Science* 1988, 242, 50.
- (15) Ovchinnikov, Yu. A. *FEBS Lett.* 1982, 148, 179.
- (16) Nathans, J.; Hogness, D. *Cell* 1983, 34, 807.
- (17) (a) Shobert, B.; Lanyi, J. K.; Oesterhelt, D. *J. Biol. Chem.* 1986, 261, 2690. (b) Jay, D.; Cantley, L. *Annu. Rev. Biochem.* 1986, 55, 511.
- (18) Green, N. M.; Taylor, W. R.; MacLeenan, D. H. *The Ion Pumps: Structure, Function and Regulation*; Stein, W., Ed.; Alan Liss Inc.: New York, 1988; p 15.

- (19) Walker, J. E.; Saraste, M.; Gay, N. J. *Biochim. Biophys. Acta* 1984, 768, 164.
- (20) Popot, J. L.; DeVitry, C. *Ann. Rev. Biophys. Biophys. Chem.* 1990, 19, 369.
- (21) Kühlbrandt, W. *Q. Rev. Biophys.* 1988, 21, 4.
- (22) Deisenhofer, J.; Epp, O.; Miki, K.; Huber, R.; Michel, H. *Nature* 1985, 318, 618.
- (23) Rees, D. C.; Komiya, H.; Yeates, T. O.; Allen, J. P.; Feher, G. *Annu. Rev. Biochem.* 1989, 58, 607.
- (24) Henderson, R.; Unwin, P. N. T. *Nature* 1975, 257, 28.
- (25) Henderson, R.; Baldwin, J. M.; Ceska, T. A.; Zemlin, F.; Beckmann, E.; Downing, K. H. *J. Mol. Biol.* 1990, 213, 899.
- (26) Moore, C.; Pressman, B. C. *Biochem. Biophys. Res. Commun.* 1964, 15, 562.
- (27) Pressman, B. C. *Proc. Natl. Acad. Sci. U.S.A.* 1965, 53, 1076.
- (28) Pressman, B. C.; Harris, E. J.; Jagger, W. S.; Johnson, J. H. *Proc. Natl. Acad. Sci. U.S.A.* 1967, 58, 1949.
- (29) Mueller, P.; Rudin, D. O. *Nature* 1968, 217, 713.
- (30) An exhaustive survey of the early literature can be found in the following: Proceedings of Molecular Mechanisms of antibiotic action on protein biosynthesis and membranes, Granada; Munoz, E., Garcia-Ferrandiz, F., Vasquez, D., Eds.; Elsevier: Amsterdam, 1972.
- (31) Ovchinnikov, Yu. A.; Ivanov, V. T.; Shkrob, A. M. *Membrane-active complexes*; BBA Library, Elsevier: Amsterdam, 1974; Vol. 12.
- (32) Simon, W.; Morf, W. E.; Meyer, P. Ch. *Structure and Bonding*; Springer-Verlag: Berlin, 1973; Vol. 16, p 113.
- (33) Sankaram, M. B.; Easwaran, K. R. K. *Magnetic Resonance in Biology and Medicine*; Govil, G., Kethrapal, L., Saran, A., Eds.; Tata MacGraw Hill Publ. Co.: New Delhi, 1985; p 333.
- (34) Dobler, M. *Ionophores and their Structure*; Wiley: New York, 1981.
- (35) Antibiotics and their complexes. In *Metal Ions and their Complexes*; Sigel, H., Ed.; Marcel Dekker: New York, 1985; Vol. 19.
- (36) Pedersen, C. J. *J. Am. Chem. Soc.* 1967, 89, 2945; 7017.
- (37) Cram, J. *Science* 1983, 219, 1177.
- (38) Lehn, J. M. *Science* 1985, 227, 849.
- (39) (a) Sarges, R.; Witkop, B. *J. Am. Chem. Soc.* 1964, 86, 1862. (b) Meyer, C. E.; Reusser, F. *Experientia* 1967, 23, 85. (c) Nagaraj, R.; Balaram, P. *Acc. Chem. Res.* 1981, 14, 356. (d) Menestrina, G.; Voges, K. P.; Jung, G.; Boheim, G. *J. Membr. Biol.* 1986, 93, 111. (e) Molle, G.; Duclouier, H.; Dugast, J. Y.; Spach, G. *Biopolymers* 1989, 28, 273.
- (40) Tosteson, D. C.; Andreoli, T. E.; Tieffenberg, M.; Cook, P. J. *Gen. Phys.* 1968, 51, 373S.
- (41) Urry, D. W. *Proc. Natl. Acad. Sci. U.S.A.* 1971, 68, 672.
- (42) Urry, D. W.; Goodall, M. C.; Glickson, J. D.; Mayers, D. F. *Proc. Natl. Acad. Sci. U.S.A.* 1971, 68, 1907.
- (43) Fox, R. O.; Richards, F. M. *Nature* 1982, 300, 325.
- (44) Boheim, G.; Hanke, W.; Jung, G. *Biophys. Struct. Mech.* 1983, 9, 181.
- (45) Hall, J. E.; Vodyanov, I.; Balasubramanian, T. M.; Marshall, G. R. *Biophys. J.* 1983, 45, 233.
- (46) De Kruijff, B.; Demel, R. A. *Biochim. Biophys. Acta* 1974, 339, 57.
- (47) Finkelstein, A.; Holz, R. *Membranes*; Eisenman, Ed.; M. Dekker Inc.: New York, 1973; Vol. 2, p 377.
- (48) Ovchinnikov, Yu. A.; Ivanov, V. T.; Evstratov, A. V.; Bystrov, V. F.; Abdulleev, N. D.; Popov, E. M.; Lipkind, G. M.; Arkhipova, S. F.; Efremov, E. S.; Shemyakin, M. M. *Biochem. Biophys. Res. Commun.* 1969, 37, 668.
- (49) Popov, E. M.; Pletnev, V. Z.; Evstratov, A. V.; Ivanov, V. T.; Ovchinnikov, Yu. A. *Kim. Prir. Soedin.* 1970, 5, 505.
- (50) Maigret, B.; Pullman, B. *Biochem. Biophys. Res. Commun.* 1973, 50, 908.
- (51) Pullman, A. *Molecular and Quantum Pharmacology*. Proceedings of the 7th Jerusalem Symposium on Quantum Chemistry and Biochemistry; Bergmann, E., Pullman, B., Eds.; Reidel: Dordrecht, 1974; p 401.
- (52) Perricaudet, M.; Pullman, A. *Int. J. Pept. Protein Res.* 1973, 5, 99.
- (53) (a) Perricaudet, M.; Pullman, A. *FEBS Lett.* 1973, 34, 222. (b) Schuster, P.; Jakubetz, W.; Marius, M. *Top. Curr. Chem.* 1975, 60, 1.
- (54) Staley, R. H.; Beauchamp, J. L. *J. Am. Chem. Soc.* 1975, 97, 5920.
- (55) (a) Pullman, A. *Physical Chemistry of Transmembrane Ion Motions*; Spach, G., Ed.; Elsevier Science Publishers: Amsterdam, 1983; p 153. (b) Welti, M.; Pretsch, E.; Clementi, E.; Simon, W. *Helv. Chim. Acta* 1982, 65, 1996.
- (56) Gresh, N.; Claverie, P.; Pullman, A. *Int. J. Quantum Chem.* 1979, 13, 243.
- (57) Gresh, N.; Etchebest, C.; de la Luz Rojas, O.; Pullman, A. *Int. J. Quantum Chem., Quantum Biol. Symp.* 1981, 8, 109.
- (58) (a) Gresh, N.; Pullman, A. *Int. J. Quantum Chem.* 1982, 22, 709. (b) Pretsch, E.; Vasak, M.; Simon, W. *Helv. Chim. Acta* 1972, 55, 1098. (c) Nawata, Y.; Sakamaki, T.; Titaka, Y. *Chem. Lett. Jpn.* 1975, 151.
- (59) Gresh, N.; Pullman, A. *Int. J. Quantum Chem., Quantum Biol. Symp.* 1983, 10, 215.
- (60) Pullman, A. *Specificity in Biological Interactions*; Pontificiae Academiae Scientiarum Scripta Varia: Vatican City, 1984; Vol. 55, p 303.
- (61) (a) Eisenman, G.; Krasne, S.; Ciani, S. *Ann. N. Y. Acad. Sci. U.S.A.* 1975, 34, 264. (b) Diebler, H.; Eigen, M.; Ilgenfritz, G.; Maass, G.; Winkler, R. *Pure Appl. Chem.* 1969, 20, 93.
- (62) Lutz, W.; Früh, P.; Simon, W. *Helv. Chim. Acta* 1971, 54, 2767.
- (63) Morf, W.; Simon, W. *Helv. Chim. Acta* 1971, 54, 794, 2683.
- (64) Neupert-Laves, K.; Dobler, M. *Helv. Chim. Acta* 1975, 58, 432.
- (65) Lavery, R.; Parker, I.; Kendrick, J. *J. Biomol. Struct. Dyn.* 1986, 4, 443.
- (66) Ovchinnikov, Yu. A.; Ivanov, I. V.; Skhrob, A. M. Proceedings of Molecular Mechanisms of antibiotic action on protein biosynthesis and membranes, Granada; Munoz, E., Garcia-Ferrandiz, F., Vasquez, D., Eds.; Elsevier: Amsterdam, 1972; p 459.
- (67) Grell, E.; Funck, R.; Sauter, H. *Eur. J. Biochem.* 1973, 34, 415.
- (68) Ovchinnikov, Yu. A.; Ivanov, V. T. *Tetrahedron* 1974, 30, 1871.
- (69) Grell, E.; Funck, Th.; Egger, F. Proceedings of Molecular Mechanisms of antibiotic action on protein biosynthesis and membranes, Granada; Munoz, E., Garcia-Ferrandiz, F., Vasquez, D., Eds.; Elsevier: Amsterdam, 1972; p 646.
- (70) (a) Shemyakin, M. M.; Ovchinnikov, Yu. A.; Ivanov, V. T.; Antonov, V. K.; Vinogradova, E. I.; Skhrob, A. M.; Malenkov, G. G.; Evstratov, A. V.; Melnik, E. I.; Ryabova, I. D. *J. Membr. Biol.* 1969, 1, 402. (b) Eisenman, G. *Biophys. J.* 1962, 2, part 2, 259. (c) Eisenman, G. *Mass transfer and kinetics on ion exchange*; Liberti, L., Helfferich, F. G., Eds.; NATO ASI series, Martinus Nijhoff Publ.: The Hague, 1983; p 121-155.
- (71) Noyes, R. M. *J. Am. Chem. Soc.* 1962, 84, 513.
- (72) Halliwell, H.; Nyburg, S. *Trans. Faraday Soc.* 1963, 59, 1126.
- (73) Cotton, F. A.; Wilkinson, G. *Advanced Inorganic Chemistry*, 3rd ed.; Interscience: New York, 1972; p 645.
- (74) Kaufmann, E.; Lehn, J. M.; Sauvage, J. P. *Helv. Chim. Acta* 1976, 59, 1099.
- (75) Lifson, S.; Felder, C. E.; Shanzer, A. *J. Biomol. Struct. Dyn.* 1984, 2, 641.
- (76) Dobler, M.; Phizakerley, R. *Helv. Chim. Acta* 1974, 54, 664.
- (77) Kilbourn, B.; Dunitz, J.; Pioda, L.; Simon, W. *J. Mol. Biol.* 1967, 1, 346.
- (78) Dobler, M.; Dunitz, J.; Kilbourn, B. *Helv. Chim. Acta* 1969, 52, 2573.
- (79) Gresh, N.; Pullman, A. *Nouv. J. Chim.* 1986, 10, 57.
- (80) Pressman, B. *Annu. Rev. Biochem.* 1976, 45, 501.
- (81) Lifson, S.; Felder, C. E.; Shanzer, A. *Biochemistry* 1984, 23, 2577.
- (82) Steinrauf, L. K.; Hamilton, J. A.; Sabesan, H. N. *J. Am. Chem. Soc.* 1982, 104, 4085.
- (83) Hamilton, J. A.; Sabesan, M. N.; Steinrauf, L. K. *J. Am. Chem. Soc.* 1981, 103, 5880.
- (84) Gresh, N.; Pullman, A. *Nouv. J. Chim.* 1986, 10, 405.
- (85) Etchebest, C.; Lavery, R.; Pullman, A. *Stud. Biophys.* 1982, 90, 7.
- (86) Smith, G. D.; Duax, W. L.; Langs, D. A.; De Titta, G. T.; Edmonds, J. W.; Rohrer, D. C.; Weeks, C. M. *J. Am. Chem. Soc.* 1975, 97, 7242.
- (87) Masut, R. E.; Kushick, N. *J. Comput. Chem.* 1984, 5, 336.
- (88) Brasseur, R.; Deleers, M. *Proc. Nat. Acad. Sci. U.S.A.* 1984, 81, 3370.
- (89) Khutorskij, V. E.; Kamenchuk, A. A.; Shchechkin, I. E. *Teoreticheskaya i Experimentalnaya Khimiya*; Plenum Publishing Corp.: New York, 1987; Vol. 23, p 360.
- (90) (a) Khutorsky, V. E.; Kamenchuk, A. A.; Alieva, I. N. *Biol. Membr.* 1987, 4, 756. (b) Wipff, G.; Weiner, P.; Kollman, P. *J. Am. Chem. Soc.* 1982, 104, 3249. (c) Gehin, D.; Kollman, P. A.; Wipff, G. *J. Am. Chem. Soc.* 1989, 111, 3011. (d) Ranghino, C.; Romano, S.; Lehn, J. M.; Wipff, G. *J. Am. Chem. Soc.* 1985, 107, 7873. (e) Lybrand, T. P.; McCammon, J. A.; Wipff, G. *Proc. Natl. Acad. Sci. U.S.A.* 1986, 83, 833. (f) Wipff, G.; Wurtz, J. M. *Transport through Membranes: Carriers, Channels and Pumps*; Pullman, A., Pullman, B., Jortner, J., Eds.; Kluwer Acad. Publishers: New York, 1988; p 1. (g) Owenson, B.; McElroy, R. D.; Pohorille, A. *J. Am. Chem. Soc.* 1988, 110, 6992. (h) Kollman, P. A.; Wipff, G.; Chandra Singh, U. *J. Am. Chem. Soc.* 1985, 107, 2212.
- (91) Venkatachalam, C. M.; Urry, D. W. *J. Comput. Chem.* 1983, 4, 461.
- (92) Urry, D. W.; Venkatachalam, C. M.; Prasad, K. U.; Bradley, R. J.; Parenti-Castelli, G.; Lenaz, G. *Int. J. Quantum Chem., Quantum Biol. Symp.* 1981, 8, 385.
- (93) Pullman, A.; Etchebest, C. *FEBS Lett.* 1983, 163, 199.
- (94) Koeppe, R. E.; Kimura, M. *Biopolymers* 1984, 23, 23.

- (95) Urry, D. W. Private communication.
- (96) Etchebest, C.; Pullman, A. *FEBS Lett.* 1984, 170, 191.
- (97) Etchebest, C.; Pullman, A. *J. Biomol. Struct. Dyn.* 1986, 3, 805.
- (98) Pullman, A.; Etchebest, C. *Ion Transport through Membranes*; Yagi, K., Pullman, B., Eds.; Academic Press: Tokyo, 1987; p 277.
- (99) Pullman, A. *Q. Rev. Biophys.* 1987, 20 (3/4), 173.
- (100) Arseniev, A. S.; Lomize, A. L.; Barsukov, I. L.; Bystrov, V. F. *Biol. Membr.* 1986, 3, 1077.
- (101) (a) Luger, P. *J. Membr. Biol.* 1980, 57, 163. (b) Finkelstein, A.; Andersen, O. S. *J. Membr. Biol.* 1981, 59, 155.
- (102) (a) Levitt, D. G. *Biophys. J.* 1978, 22, 209. (b) Luger, P. *Biophys. Chem.* 1982, 15, 89. (c) Fischer, W.; Brickmann, J.; Luger, P. *Biophys. Chem.* 1981, 13, 105.
- (103) Polymeropoulos, E. E.; Brickmann, J. *Annu. Rev. Biophys., Biophys. Chem.* 1985, 14, 315.
- (104) (a) Jordan, P. C. *Biophys. J.* 1987, 51, 661. (b) Kee Lee, W.; Jordan, P. C. *Biophys. J.* 1984, 46, 805. (c) Sung, S. S.; Jordan, P. C. *J. Phys. Chem.* 1988, 92, 2362. (d) Sung, S. S.; Jordan, P. C. *Biophys. J.* 1987, 51, 661. (e) Jordan, P. C. *Biophys. J.* 1991, 59, 320a.
- (105) Schroder, H. *Eur. Biophys. J.* 1985, 12, 129.
- (106) Pullman, A.; Etchebest, C. *FEBS Lett.* 1983, 163, 199.
- (107) Etchebest, C.; Ranganathan, S.; Pullman, A. *FEBS Lett.* 1984, 173, 301.
- (108) Etchebest, C.; Pullman, A. *J. Biomol. Struct. Dyn.* 1985, 2, 259.
- (109) Etchebest, C.; Pullman, A. *J. Biomol. Struct. Dyn.* 1988, 5, 1111.
- (110) Etchebest, C.; Pullman, A. *FEBS Lett.* 1986, 204, 365.
- (111) Etchebest, C.; Pullman, A.; Ranganathan, S. *Biochim. Biophys. Acta* 1985, 818, 23.
- (112) Etchebest, C.; Pullman, A. *FEBS Lett.* 1986, 204, 261.
- (113) (a) Mazet, J. L.; Andersen, O. S.; Koeppe, R. E., II. *Biophys. J.* 1984, 45, 263. (b) Barrett-Russel, E. W.; Weiss, L. B.; Navetta, F. I.; Koeppe, R. E.; Andersen, O. S. *Biophys. J.* 1986, 49, 673. (c) Koeppe, R. E., II; Mazet, J. L.; Andersen, O. S. *Biochemistry* 1990, 29, 512. (d) Brenneeman, M.; Chiu, S. W.; Jakobsson, E. *Biophys. J.* 1991, 59, 320a.
- (114) (a) Heitz, F.; Dumas, P.; Van Mau, N.; Lazaro, R.; Trudelle, Y.; Etchebest, C.; Pullman, A. *Transport through Membranes: Carriers, Channels and Pumps*; Pullman, A., Pullman, B., Jortner, J., Eds.; Kluwer Academic Publishers: New York, 1988; p 147. (b) Heitz, F.; Gavach, C.; Spach, G.; Trudelle, Y. *Biophys. Chem.* 1986, 24, 143. (c) Heitz, F.; Dumas, P.; Van Mau, N.; Trudelle, Y. *Biophys. J.* 1988, 53, 3270. (d) Becker, M. D.; Koeppe, R. E., II; Andersen, O. S. *Biophys. J.* 1991, 59, 322a. (e) Wang, J.; Pullman, A. *Chem. Phys. Lipids* 1991, 57, 1; *Biochim. Biophys. Acta* 1990, 1024, 10.
- (115) Eisenman, G.; Horn, R. *J. Membr. Biol.* 1983, 76, 197.
- (116) Eisenmann, G.; Sandblom, J. P. *Physical Chemistry of Transmembrane Ion Motions*; Spach, G., Ed.; Elsevier Science Publishers: Amsterdam, 1983; p 329.
- (117) McKay, H. J.; Berens, P. H.; Wilson, H. R.; Hagler, A. T. *Biophys. J.* 1984, 46, 229.
- (118) (a) McKay, H. J., Ph.D. Thesis, University of California, San Diego, 1985. (b) Skerra, A.; Brickmann, J. *Biophys. J.* 1987, 51, 969; 977.
- (119) Urry, D. W.; Prasad, K. U.; Trapane, T. L. *Proc. Acad. Sci. U.S.A.* 1982, 79, 390.
- (120) Urry, D. W.; Venkatachalam, C. M.; Spisni, A.; Luger, P.; Khaled, Md. A. *Proc. Natl. Acad. Sci. U.S.A.* 1980, 77, 2028.
- (121) Urry, D. W.; Trapane, T. L.; Brown, R. A.; Venkatachalam, C. M.; Prasad, K. U. *J. Magn. Reson.* 1985, 65, 43.
- (122) (a) Urry, D. W. *Ion Transport through Membranes*; Yagi, K., Pullman, B., Eds.; Academic Press: Tokyo, 1987; p 233. (b) Ke He Huang; Huey, W.; Wu, Y. *Biophys. J.* 1991, 59, 318a. (c) Hinton, J. F.; Fernandez, J. Q.; Shungu, D. C.; Whaley, W. L.; Koeppe, R. E., II; Millet, F. S. *Biophys. J.* 1988, 54, 527. (d) Shungu, D. C.; Hinton, J. F.; Koeppe, R. E., II; Millet, F. S. *Biochemistry* 1986, 25, 6103. (e) Hinton, J. F.; Fernandez, J. Q.; Shungu, D. C.; Millet, F. S. *Biophys. J.* 1989, 55, 327.
- (123) Fornili, S. L.; Vercanteren, D. P.; Clementi, E. *J. Mol. Catal.* 1984, 23, 341.
- (124) Chiu, S. W.; Subramanian, S.; Jakobsson, E.; MacCammon, J. A. *Biophys. J.* 1989, 56, 253.
- (125) (a) For a summary, see: Andersen, O. *Annu. Rev. Physiol.* 1984, 46, 531. (b) Levitt, D. G.; Elias, S. R.; Hautman, J. M. *Biochim. Biophys. Acta* 1978, 512, 436.
- (126) Pullman, A. *Molecular Description of Biological Membrane Components by Computer-Aided Conformational Analysis*; Brasseur, R., Ed.; CRC Press Inc.: Boca Raton, FL, 1990; Vol. II, p 113.
- (127) Kim, K. S.; Clementi, E. *J. Am. Chem. Soc.* 1985, 107, 5504.
- (128) Akvist, J.; Warshel, A. *Biophys. J.* 1989, 56, 171.
- (129) Venkatachalam, C. M.; Urry, D. W. *J. Comput. Chem.* 1984, 5, 64.
- (130) Roux, B.; Karplus, M. *Biophys. J.* 1988, 53, 297.
- (131) (a) Nicholson, L. K.; LoGrasso, P. V.; Cross, T. A. *J. Am. Chem. Soc.* 1989, 111, 400. (b) Nicholson, L. K.; Cross, T. A. *Biochemistry* 1989, 28, 9379. (c) Andersen, O. S.; Providence, L. L.; Koeppe, R. E. *Biophys. J.* 1990, 57, 100a.
- (132) Busath, D.; Helmsley, G.; Bridal, T.; Pear, M.; Gaffney, K.; Karplus, M. *Transport through membranes: carriers, channels and pumps*; Pullman, A., Jortner, J., Pullman, B., Eds.; Kluwer Academic Publishers: Dordrecht, 1988; p 187.
- (133) Etchebest, C.; Pullman, A. *Transport through Membranes: Carriers, Channels and Pumps*; Pullman, A., Pullman, B., Jortner, J., Eds.; Kluwer Academic Publishers: New York, 1988; p 167.
- (134) Arseniev, A. S.; Barsukov, I. L.; Bystrov, V. F.; Lomize, A. L.; Ovchinnikov, Yu. A. *FEBS Lett.* 1985, 186, 168.
- (135) Urry, D. W.; Walker, J. T.; Trapane, T. L. *J. Membr. Biol.* 1982, 69, 225.
- (136) (a) Veatch, W. R.; Fossel, E. T.; Blout, E. R. *Biochemistry* 1974, 13, 5257. (b) Wallace, B. *Annu. Rev. Biophys. Biophys. Chem.* 1990, 19, 127 and references therein. (c) Wallace, B.; Ravikumar, K. *Science* 1988, 241, 182. (d) Langs, D. A. *Science* 1988, 241, 188. (e) Durkin, J. T.; Andersen, O. S.; Heitz, F.; Trudelle, Y.; Koeppe, R. E. II. *Biophys. J.* 1987, 51, 451a. (f) Sung, S. S.; Jordan, P. C. *Biophys. J.* 1988, 54, 519. (g) Jordan, P. C.; Bacquet, R. J.; Mc Cammon, J. A.; Phou Tran. *Biophys. J.* 1989, 55, 1041.
- (137) Furois-Corbin, S.; Pullman, A. *Biochem. Biophys. Acta* 1988, 944, 399.
- (138) Rinnert, H.; Maigret, B. *Biochem. Biophys. Res. Commun.* 1981, 101, 853.
- (139) Bergès, J.; Caillet, J.; Langlet, J.; Gresh, N.; Hervé, M.; Gary-Bobo, C. M. *Modeling of Molecular Structures and Properties in Physical and Theoretical Chemistry*; Rivail, J. L., Ed.; Elsevier Publishers: Amsterdam, 1990; Vol. 71, p 253.
- (140) Khutorsky, V. E.; Kamenchuk, A. A. *Biol. Membr.* 1988, 5, 173.
- (141) Khutorsky, V. E.; Kamenchuk, A. A.; Yermishkin, L. N. *Biophys. J.* 1988, 33, 854.
- (142) Capaldi, R. A. *Trends Biochem. Sci.* 1982, 7, 292.
- (143) Ovchinnikov, Yu. A. *Trends Biochem. Sci.* 1987, 12, 434.
- (144) Maelicke, A. *Trends Biochem. Sci.* 1988, 13, 199.
- (145) Caterall, W. A. *Annu. Rev. Biochem.* 1986, 55, 953.
- (146) (a) Numa, S. *The Harvey Lectures* 1989, 83, 121. (b) Kennedy, S. J.; Roesko, R. W.; Freeman, A. R.; Watanabe, A. M.; Besch, H. R. *Science* 1977, 196, 1341. (c) Heitz, F.; Spach, G.; Seta, P.; Gavach, C. *Biochem. Biophys. Res. Commun.* 1982, 107, 481. (d) Heitz, F.; Spach, G. *Biochem. Biophys. Res. Commun.* 1982, 105, 179. (e) Lear, J. D.; Wasserman, Z. R.; DeGrado, W. E. *Science* 1988, 240, 1177. (f) DeGrado, W. E.; Lear, J. D. *Biopolymers* 1990, 29, 205.
- (147) Pullman, A. *Pure Appl. Chem.* 1988, 60, 259.
- (148) Furois-Corbin, S.; Pullman, A. *Chem. Phys. Lett.* 1986, 123, 305.
- (149) Furois-Corbin, S.; Pullman, A. *Biochim. Biophys. Acta* 1986, 860, 165.
- (150) Furois-Corbin, S.; Pullman, A. *J. Biomol. Struct. Dyn.* 1987, 4, 589.
- (151) (a) Furois-Corbin, S.; Pullman, A. *Biochim. Biophys. Acta* 1987, 902, 31. (b) Pullman, A. *Ion Pumps*; Stein, W., Ed.; Alan Liss Inc.: New York, 1988; p 113.
- (152) (a) Eisenman, G.; Oberhauser, A.; Bezanilla, F. *Transport through membranes: carriers, channels and pumps*; Pullman, A., Jortner, J., Pullman, B., Eds.; Kluwer Academic Publishers: Dordrecht, 1988; p 27. (b) Eisenman, G.; Alvarez, O. *J. Membr. Biol.* 1991, 119, 109. (c) Oiki, S.; Danko, W.; Madison, V.; Montal, M. *Proc. Natl. Acad. Sci. U.S.A.* 1988, 85, 8703.
- (153) Wada, A. *Adv. Biophys.* 1976, 9, 1.
- (154) Changeux, J. M. *Fidia Research Foundation Neuroscience Award Lectures*; Raven Press Ltd.: New York, 1990; Vol. 4, p 21.
- (155) Giraudat, J.; Dennis, M.; Heidmann, P. Y.; Haumont, P. Y.; Lederer, F.; Changeux, J. P. *Biochemistry* 1987, 26, 2410.
- (156) Furois-Corbin, S.; Pullman, A. *Transport through Membranes: Carriers, Channels and Pumps*; Pullman, A., Jortner, J., Pullman, B., Eds.; Kluwer Academic Publishers: Dordrecht, 1988; p 337.
- (157) Furois-Corbin, S.; Pullman, A. *Biochim. Biophys. Acta* 1989, 984, 339.
- (158) Furois-Corbin, S.; Pullman, A. *FEBS Lett.* 1989, 252, 63.
- (159) Pullman, A.; Furois-Corbin, S. Proceedings of the 6th conversation in Biomolecular Stereodynamics, Structure and Methods; Sarma, R. H., Sarma, M., Eds.; Adenine Press: Guilderland, NY, 1990; Vol. 2 (DNA-Protein Complexes and Proteins), p 195.
- (160) Furois-Corbin, S.; Pullman, A. *Biophys. Chem.* 1991, 39, 153.
- (161) Pullman, A.; Furois-Corbin, S.; Andrade, A. M. *Modeling of Molecular Structure and Properties*; Rivail, J. L., Ed.; Elsevier: Amsterdam, 1990; p 527.

- (162) Eisenberg, D. *Annu. Rev. Biochem.* 1984, 53, 595.  
(163) Engelman, D. M.; Steitz, T. A.; Goldman, A. *Annu. Rev. Biophys. Chem.* 1986, 15, 321.  
(164) Popot, J. L.; Changeux, J. P. *Physiol. Rev.* 1984, 64, 1162.  
(165) Imoto, K.; Busch, C.; Sakmann, B.; Mishina, M.; Konno, T.; Nakai, J.; Bujo, H.; Mori, Y.; Fukuda, K.; Numa, S. *Nature* 1988, 335, 645.  
(166) Pullman, A. *Molecular basis of neurological disorders and their treatment*; Gorrod, J. M., Albano, O., Ferrari, E., Papa, S., Eds.; Chapman and Hall, Ltd: London, in press.